This pdf file contains all figure pages in the dissertation:

A STUDY OF A MULTI-CENTURY CORAL STABLE ISOTOPE RECORD FROM RAROTONGA, SOUTHWEST SUBTROPICAL PACIFIC, FOR THE PERIOD 1726-1997

by

Lei Ren

A Dissertation

Submitted to the University at Albany, State University of New York

in Partial Fulfillment of

the Requirements for the Degree of

Doctor of Philosophy

College of Arts & Sciences

Department of Earth & Atmospheric Sciences

2002

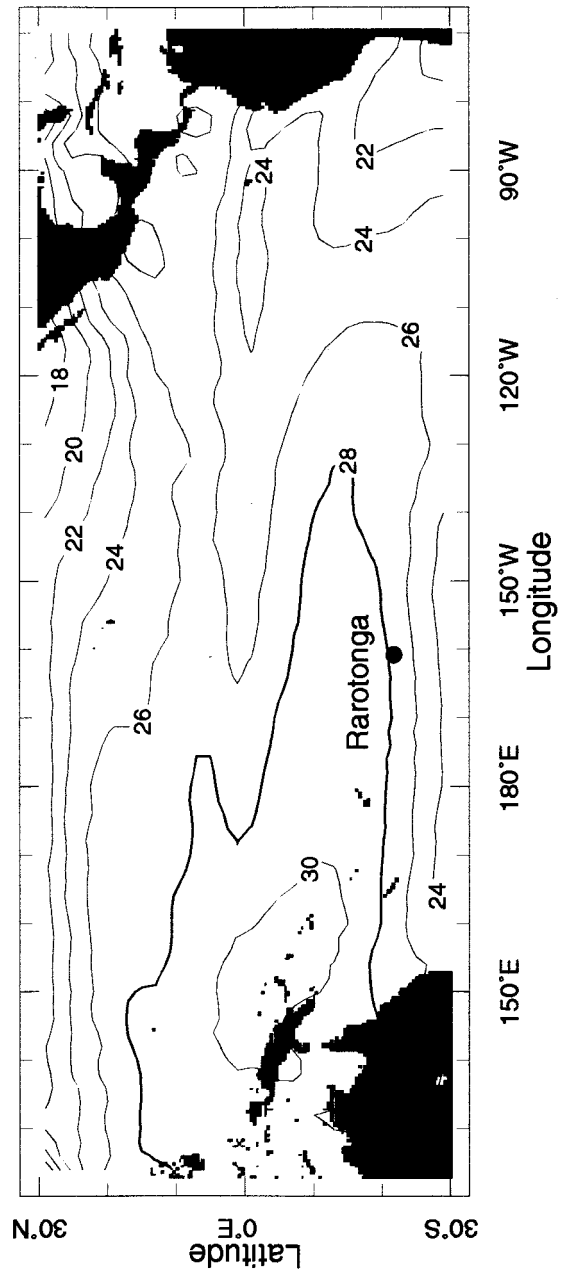

Fig. 2.1 The geographic location of Rarotonga. The contours shown are monthly averaged sea surface temperature (SST) in the Pacific. SST data is from IGOSS SST (Reynolds and Smith, 1994). The warm pool is indicated by the 28°C isotherm.

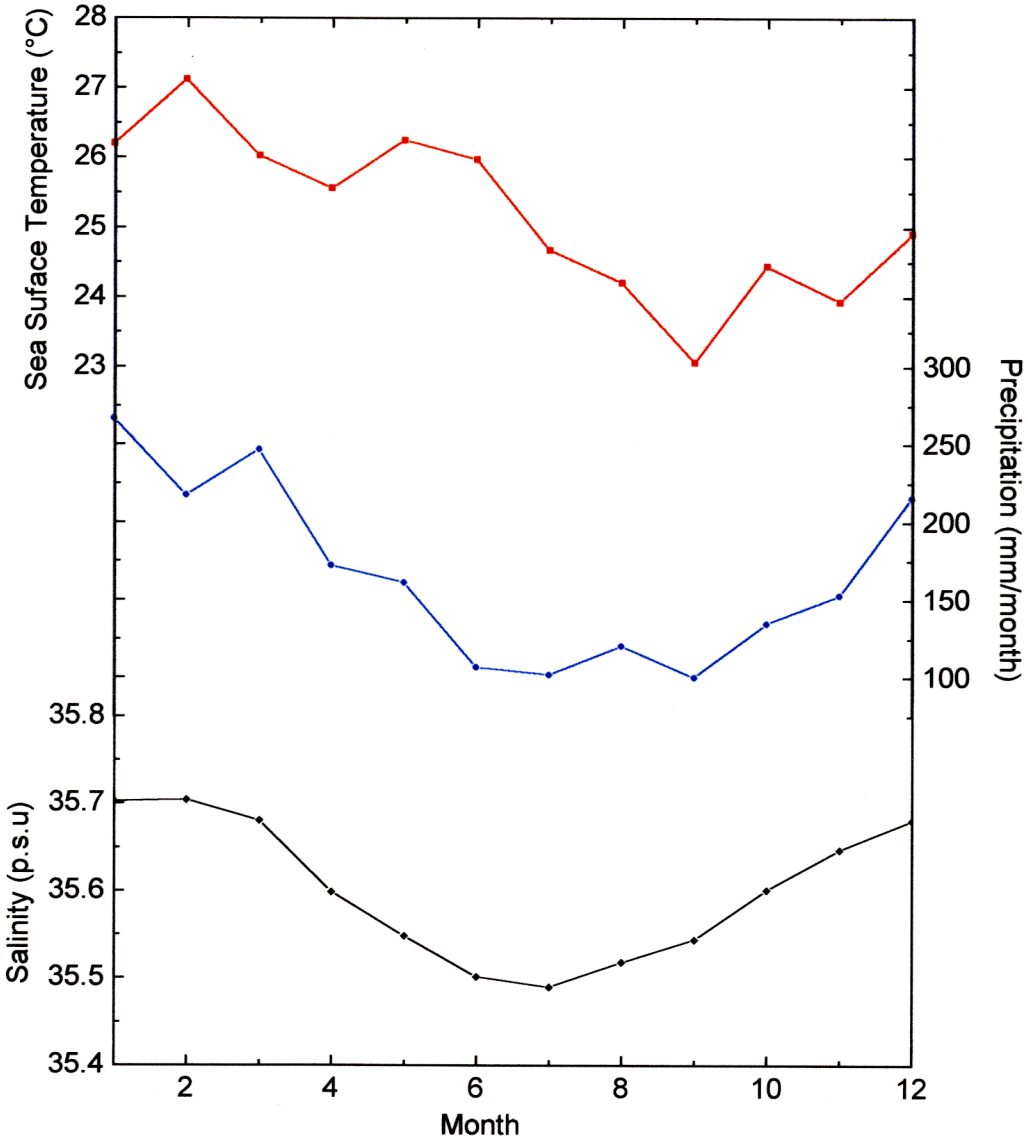

Fig. 2.2 Composite annual curves calculated by averaging monthly sea surface temperature (SST) (in red), rainfall (in blue), and salinity (at 20m depth) (in black) in the vicinity of Rarotonga for the period 1981-1997. The SST data is from IGOSS SST (Reynolds and Smith, 1994), while rainfall and salinity data are from NOAA NCDC GCPS monthly precipitation(Baker et al., 1994) and NOAA NCEP EMC CMB Pacific monthly salinity (Behringer et al., 1998; Ji et al., 1995; Ji and Smith, 1995), respectively.

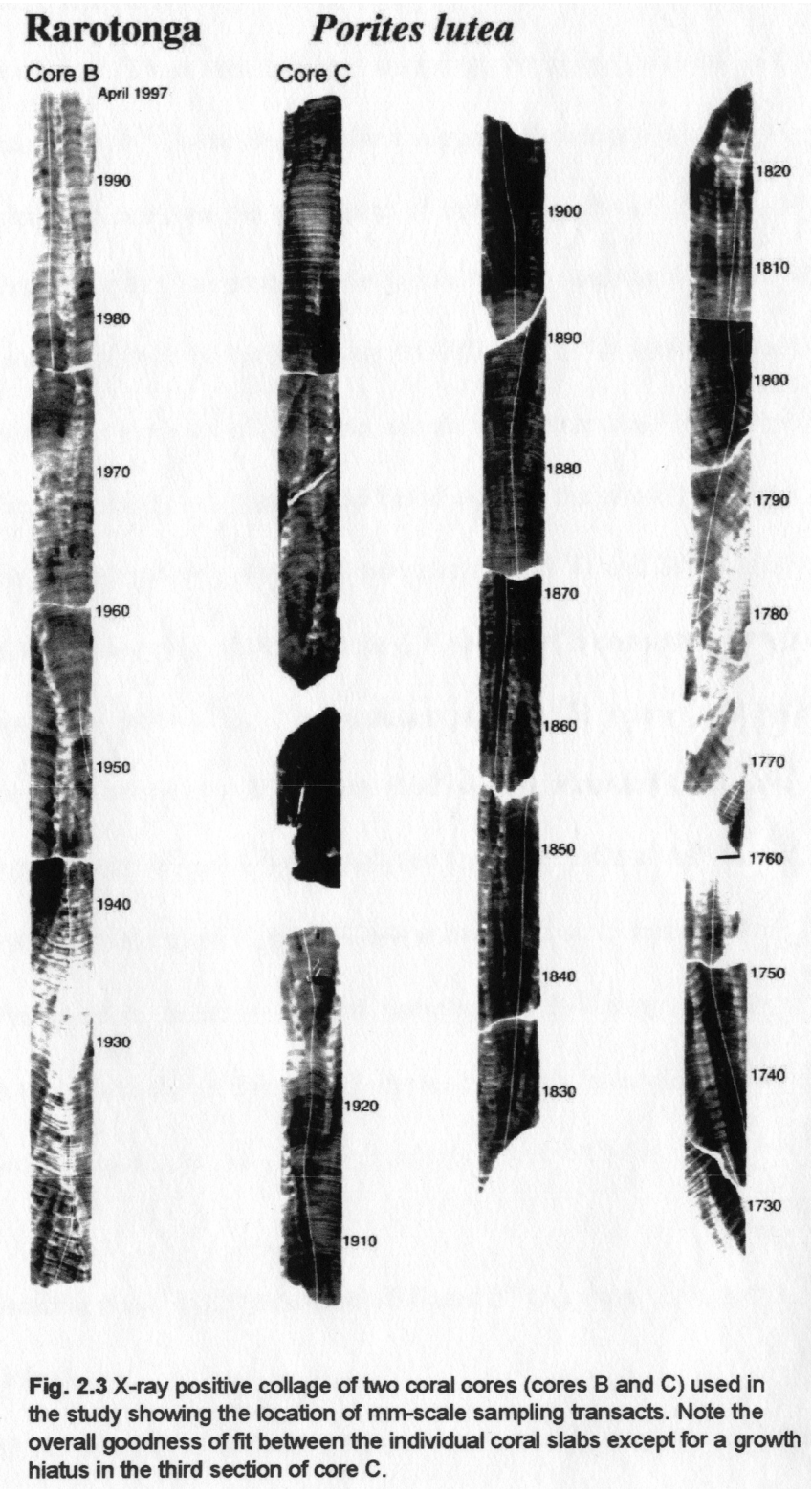

Fig. 2.3 X-ray positive collage of two coral cores (cores B and C) used in the study showing the location of mm-scale sampling transacts. Note the overall goodness of fit between the individual coral slabs except for a growth hiatus in the third section of core C.

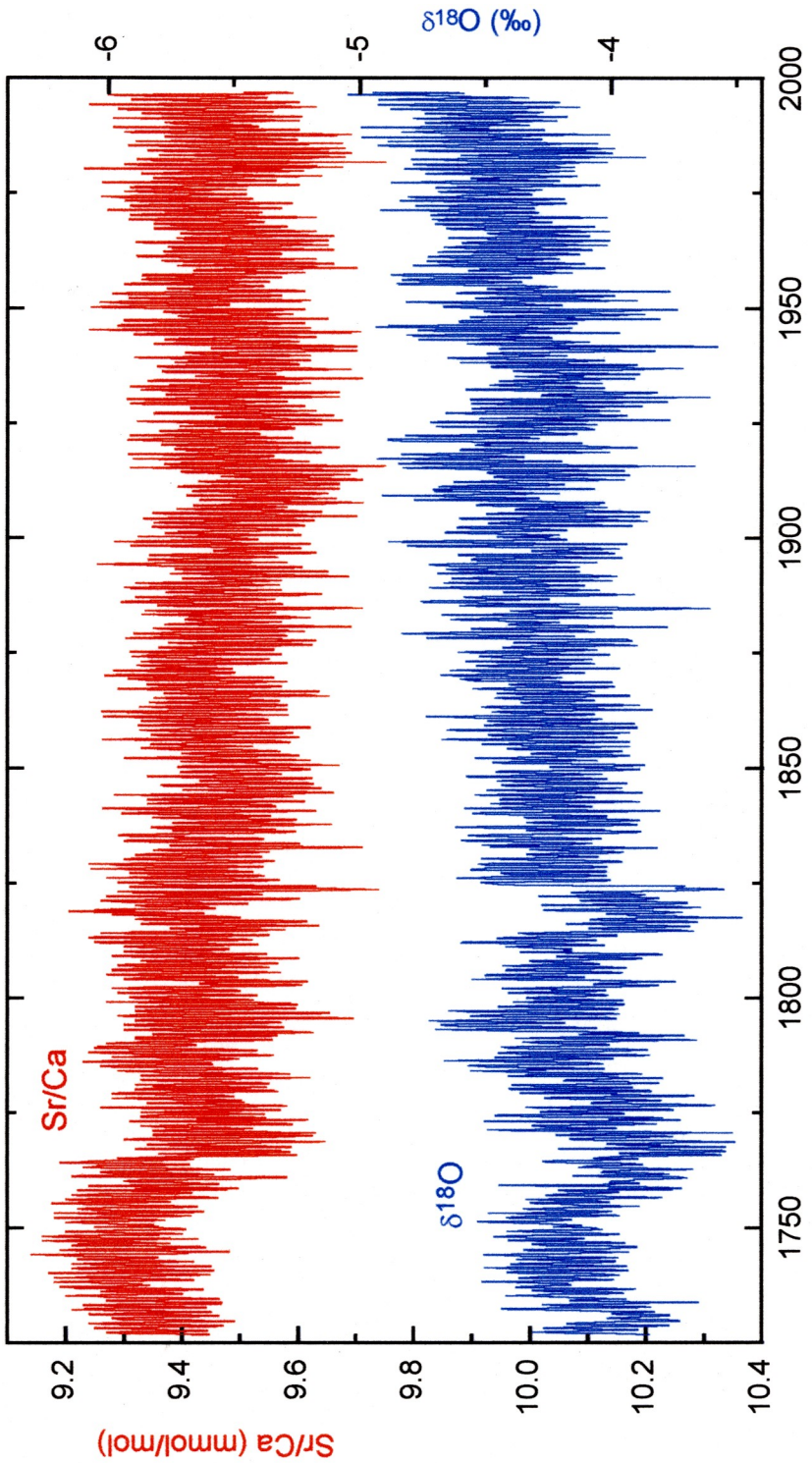

Fig. 2.4 Top curve in red: Rarotonga subseasonal Sr/Ca ratio for the period 1726-1997 (Linsley, et al., 2000a). Bottom curve in blue: Rarotonga subseasonal $\delta^{18}O$ record for the period 1726-1997.

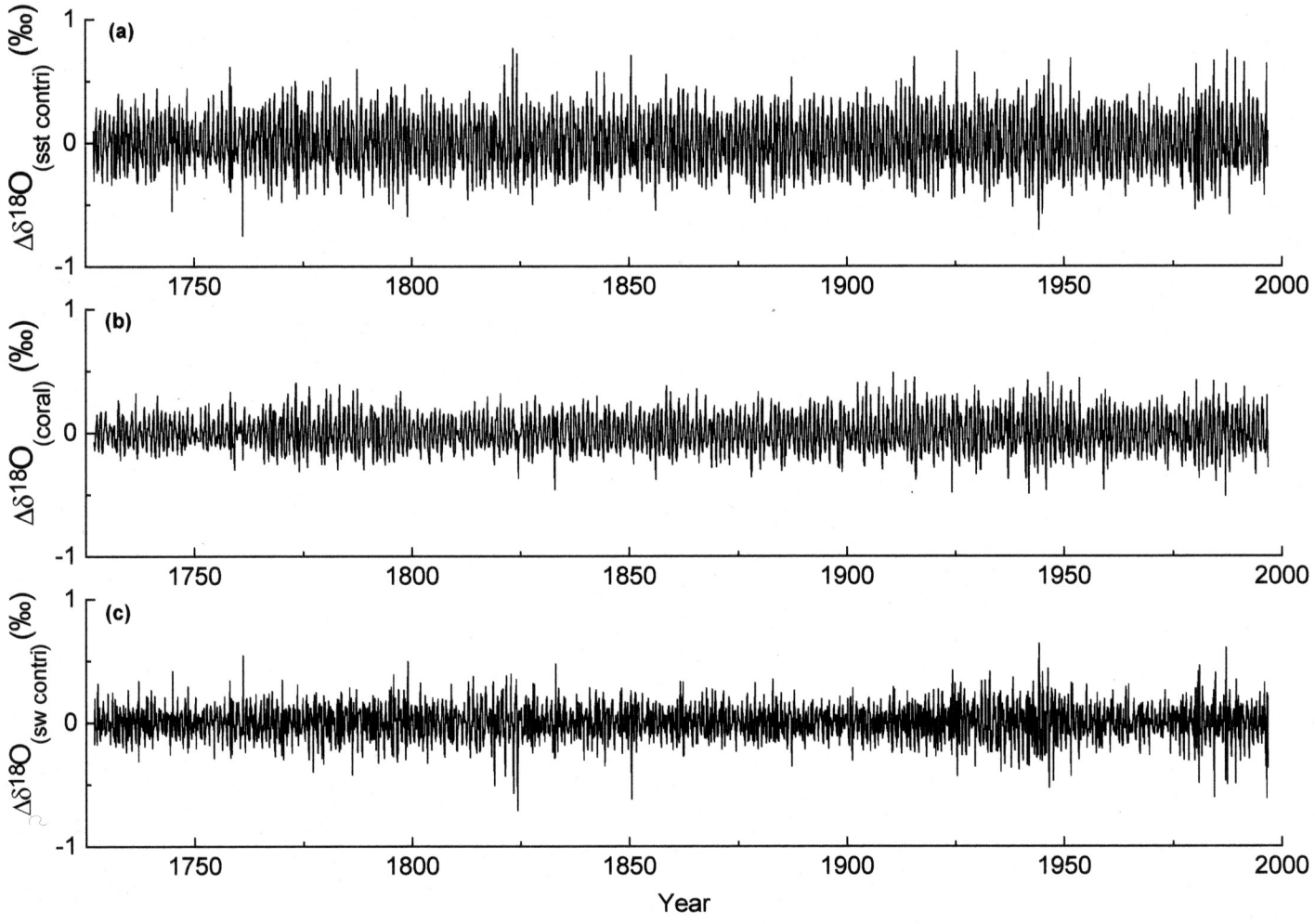

Fig. 2.5 (a) The instantaneous contribution by SST to the change of $\delta^{18}O$ in corals from Sr/Ca change for the period 1726-1997 **(b)** The instantaneous changes of $\delta^{18}O$ in corals for the period 1726-1997. **(c)** The instantaneous contribution by $\delta^{18}O_{sw}$ to the change of $\delta^{18}O$ in corals for the period 1726-1997.

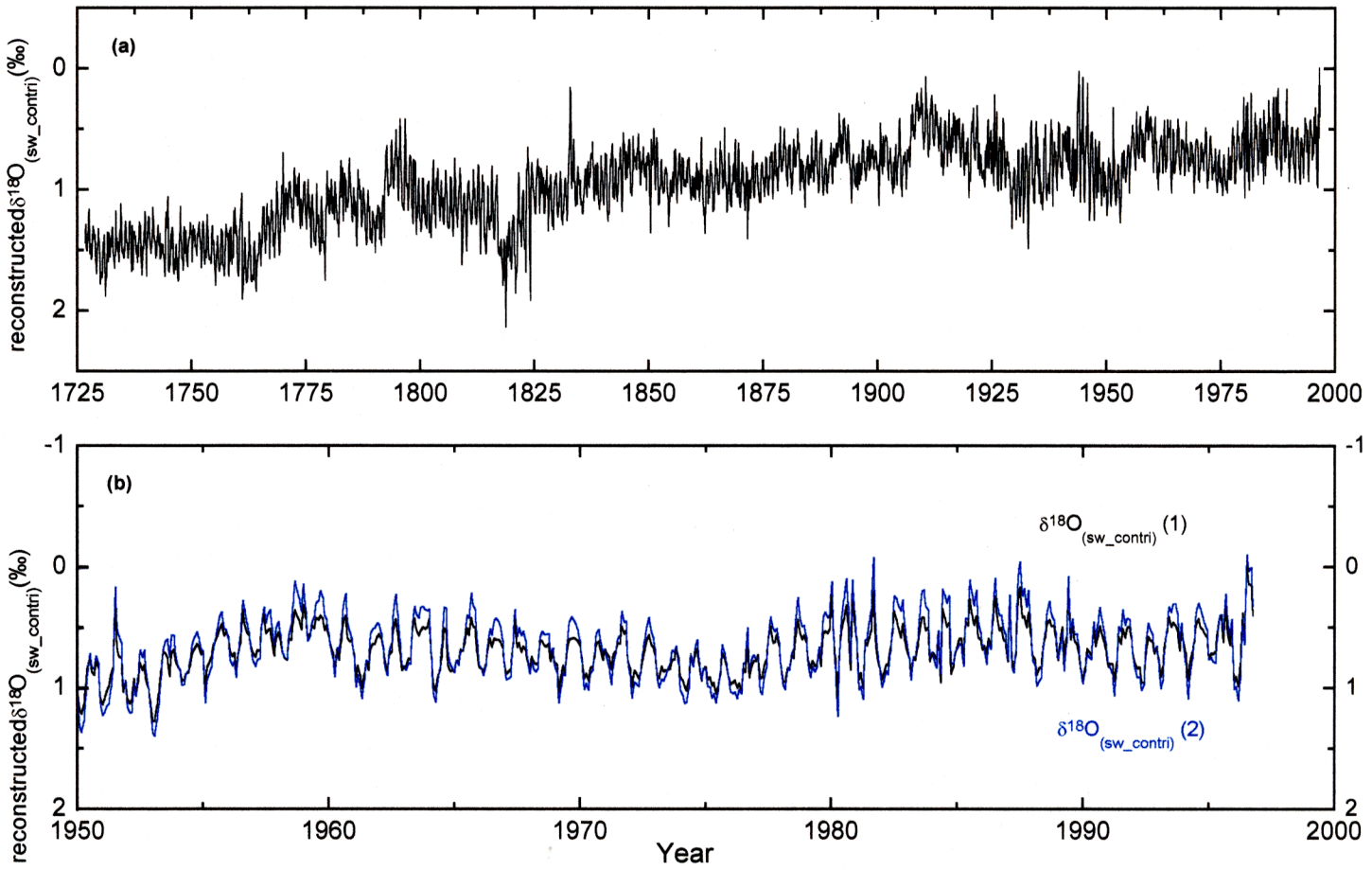

Fig. 2.6 (a) Reconstructed $\delta^{18}O_{(sw\_contri)}$ from $\delta^{18}O$ and Sr/Ca ratio in corals for the period 1726-1997. **(b)** Comparison of reconstructed $\delta^{18}O_{(sw\_contri)}$ in (a) ($\delta^{18}O_{(sw\_contri)}$ (1) in black) with the recalculated $\delta^{18}O_{(sw\_contri)}$ ($\delta^{18}O_{(sw\_contri)}$ (2) in blue) after adding the relative error of 27% (only show the portion of 1950-1997) (see text for discussion of error estimate).

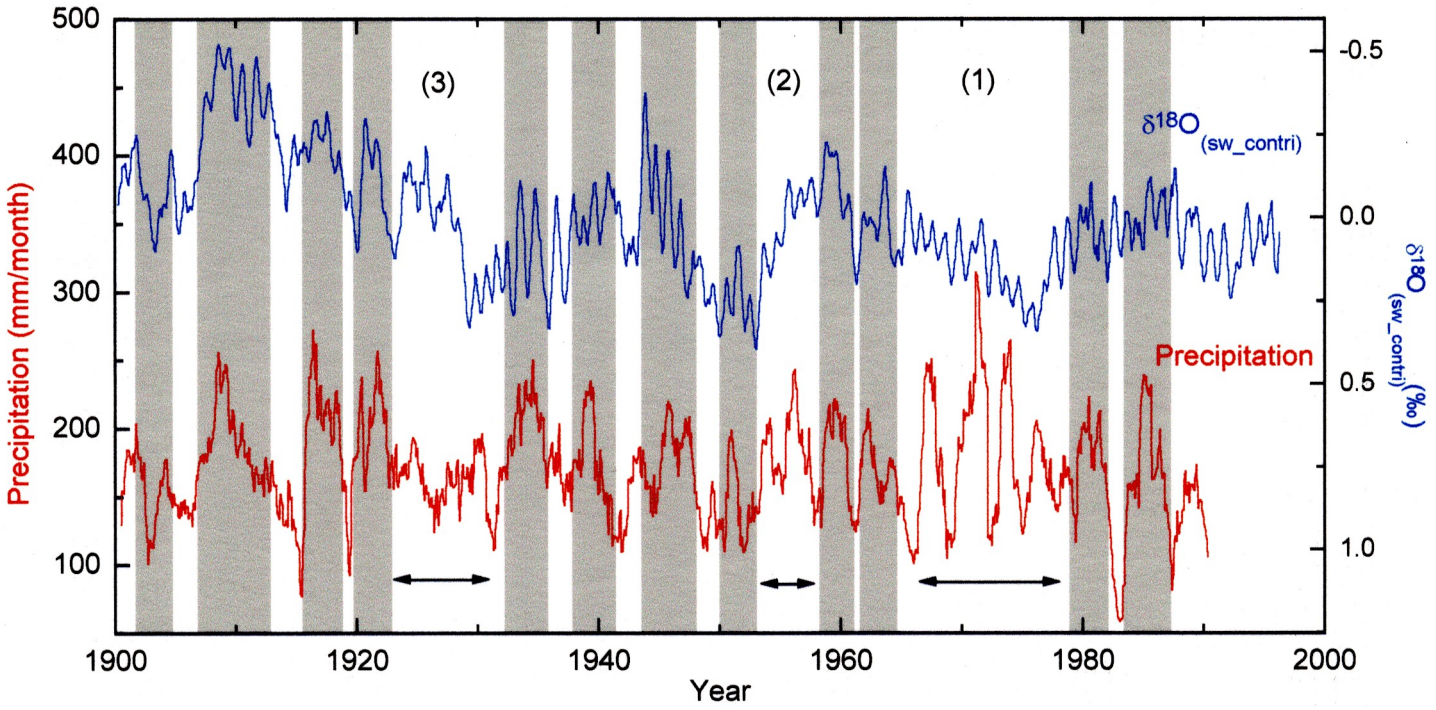

Fig. 2.7 Comparison of derived $\delta^{18}O_{(sw\_contri)}$ (in blue) and precipitation data (in red) (Baker et al., 1994) for the period 1900-1997. 1-year smooting applied on the two curves to remove the random noise. The shadows represent their similar variabilities during the same time intervals in $\delta^{18}O_{(sw\_contri)}$ and precipitation. The numbers (1)-(3) marked in the figure are the three periods that do not show very apparent similar trend between the two curves.

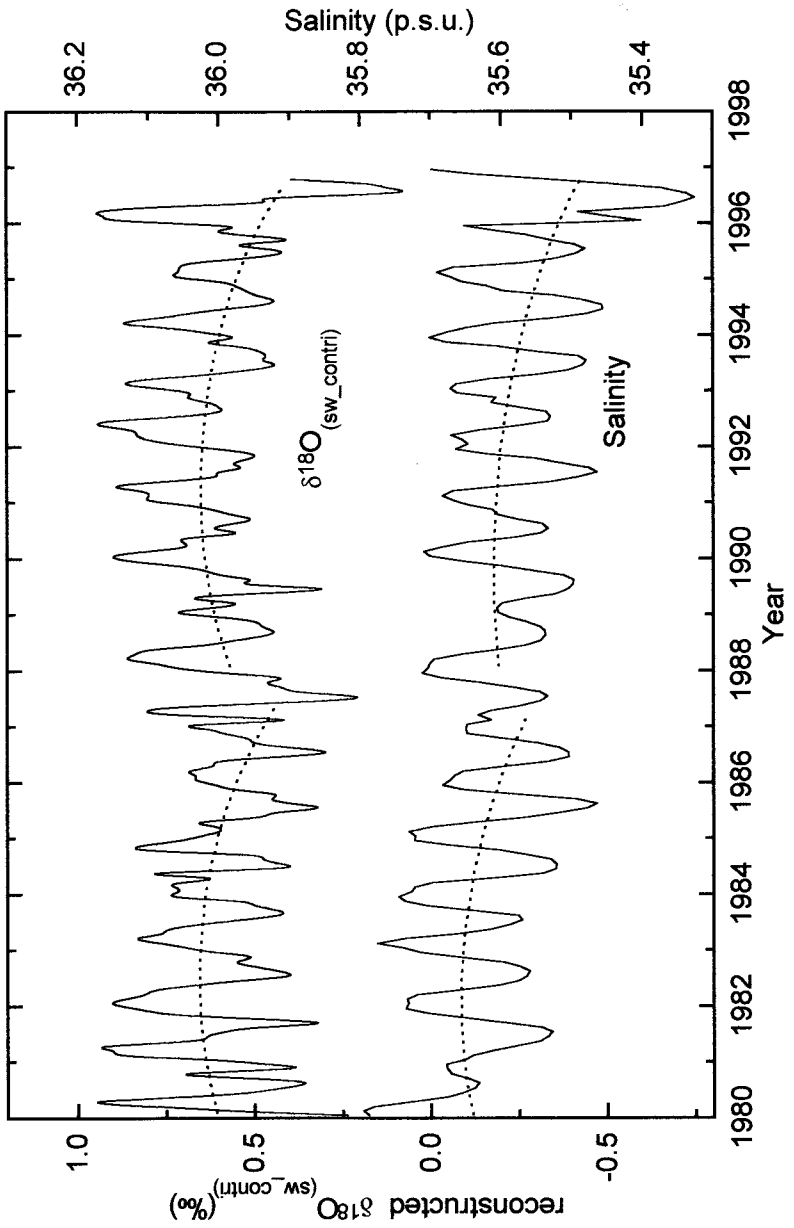

Fig. 2.8 Comparison between derived $\delta^{18}O_{(sw\_contri)}$ and salinity (Behringer, et al., 1998; Ji et al., 1995; Ji and Smith, 1995) for the period 1980-1997. The dash lines represent the potential similar trends in $\delta^{18}O_{(sw\_contri)}$ and salinity.

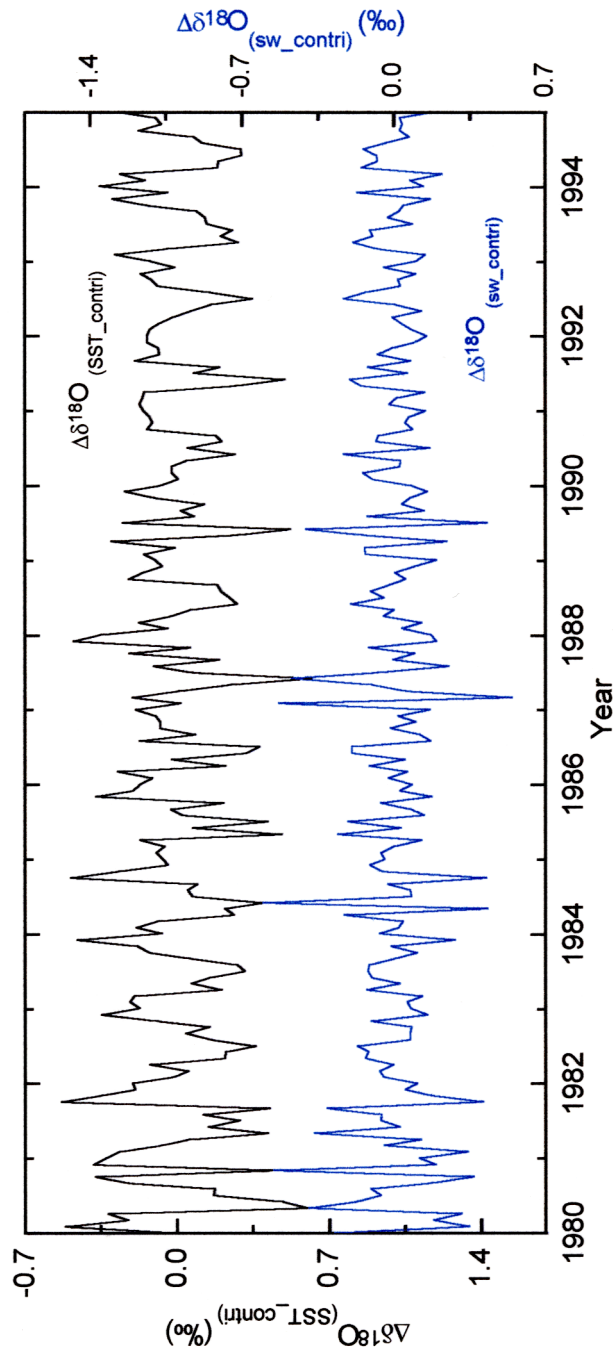

Fig. 2.9 Comparison of the instantaneous changes of the contribution from SST (in black) to the total coral $\delta^{18}O$ with that from $\delta^{18}O_{(sw\_contri)}$ (in blue) to the total coral $\delta^{18}O$ to show their opposite correlation (only shows the portion of 1980-1995).

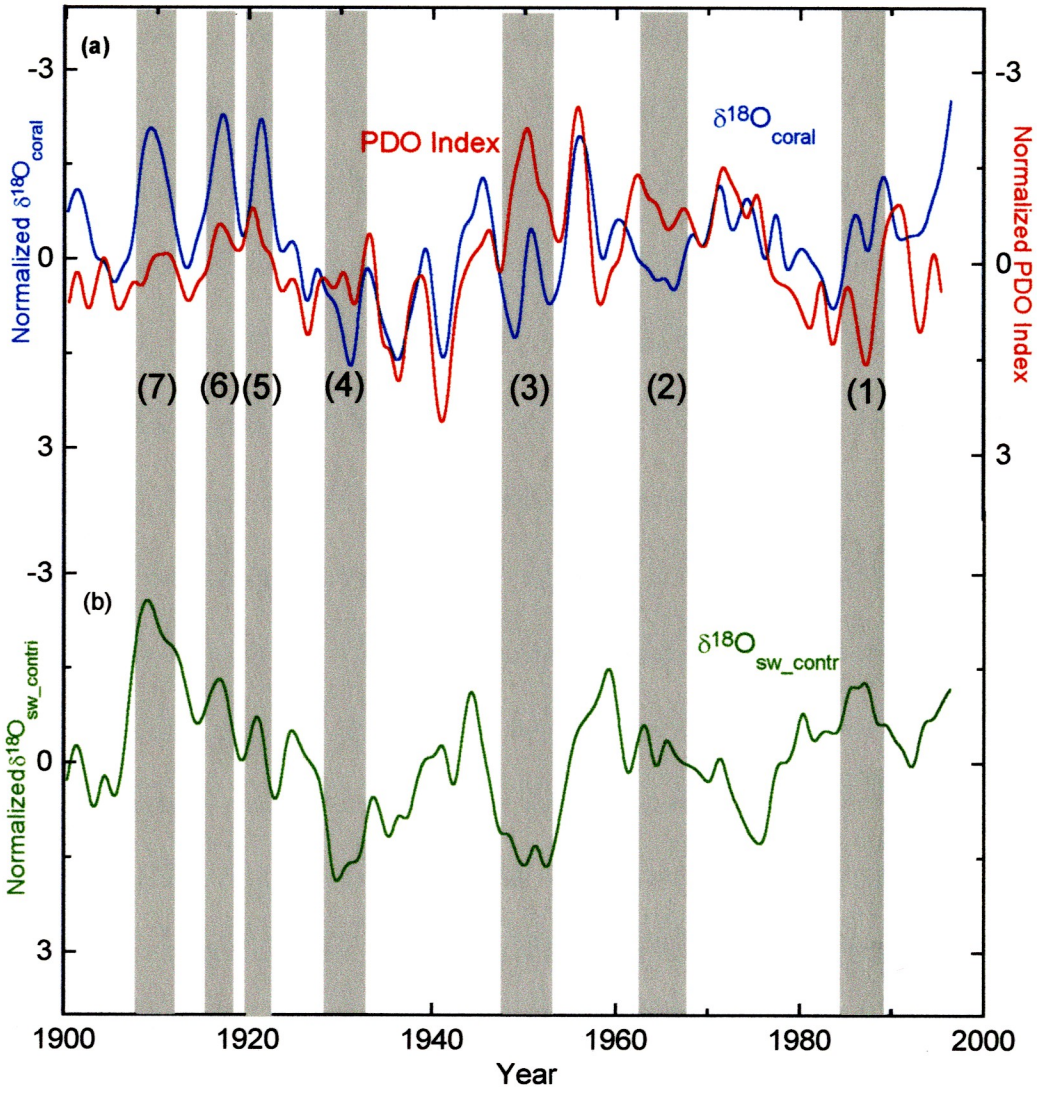

Fig. 2.10 (a) Comparison between annual average $\delta^{18}O$ (in blue) in Rarotonga corals and annual average PDO Index (in red) for the period 1900-1997. **(b)** The reconstructed annual average $\delta^{18}O_{(sw\_contri)}$ for the period 1900-1997. PDO Index, coral $\delta^{18}O$ and $\delta^{18}O_{(sw\_contri)}$ are all detrended and 5-year smoothing to highlight their decadal variability and they are all normalized in standard deviation units for comparison. The shadows marked by (1)-(7) in (a) and (b) are the time intervals that have disagreement between normalized $\delta^{18}O$ in corals and PDO Index and their corresponding changes in $\delta^{18}O_{(sw\_contri)}$.

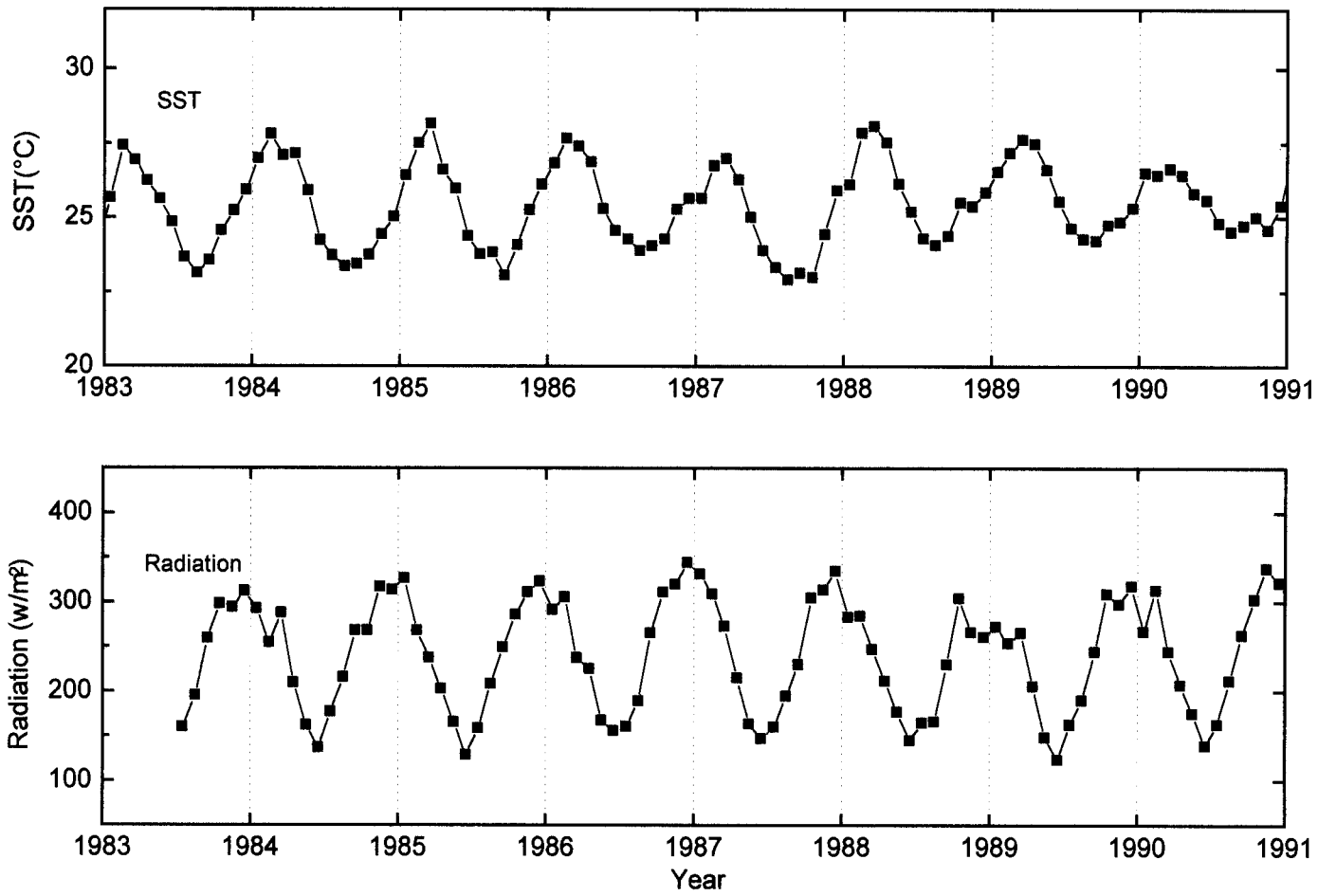

Fig. 3.1 Monthly sea surface temperature (SST), and radiation in the vicinity of Rarotonga for the period 1983-1991. The SST data is from the IGOSS data archive for the 1x1 degree latitude-longitude block (Reynolds and Smith, 1994) while radiation data is from ISCCP for 2x2 degree latitude-longitude grid surrounding Rarotonga.

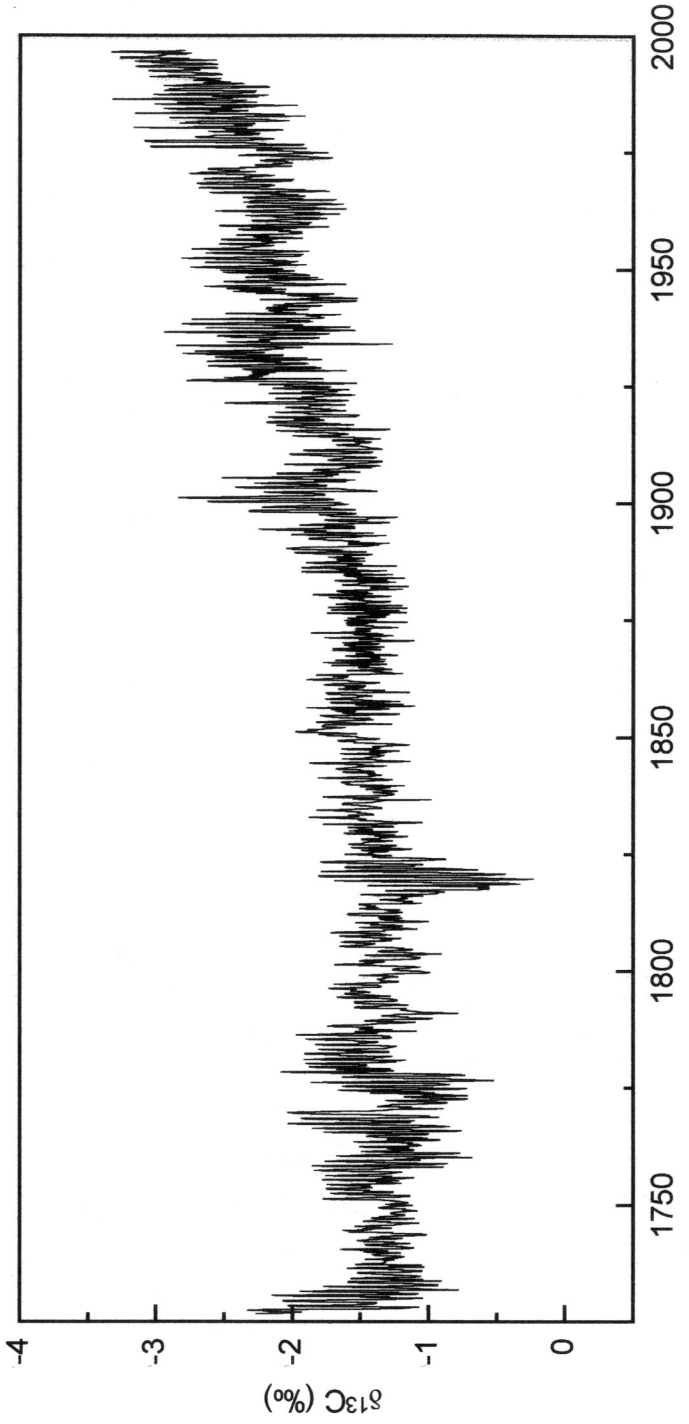

Fig. 3.2 Subseasonal $\delta^{13}C$ (relative to Peedee belemnite (PDB)) spanning 1726-1997 at Rarotonga.

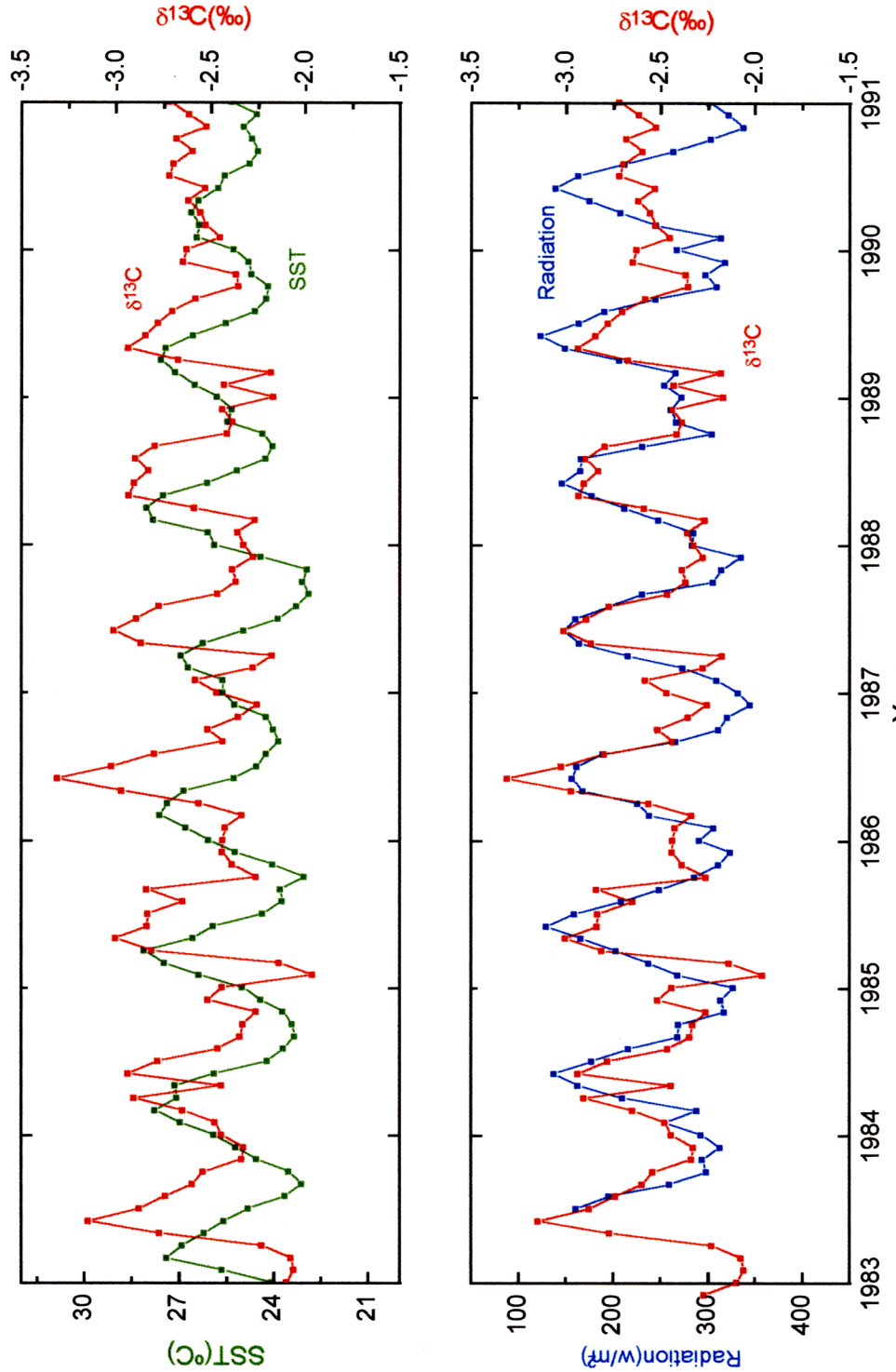

Fig. 3.3 Comparison of $\delta^{13}C$ (in red) in corals with monthly SST (in green) and radiation (in blue) data for the period 1983-1991 at Rarotonga.

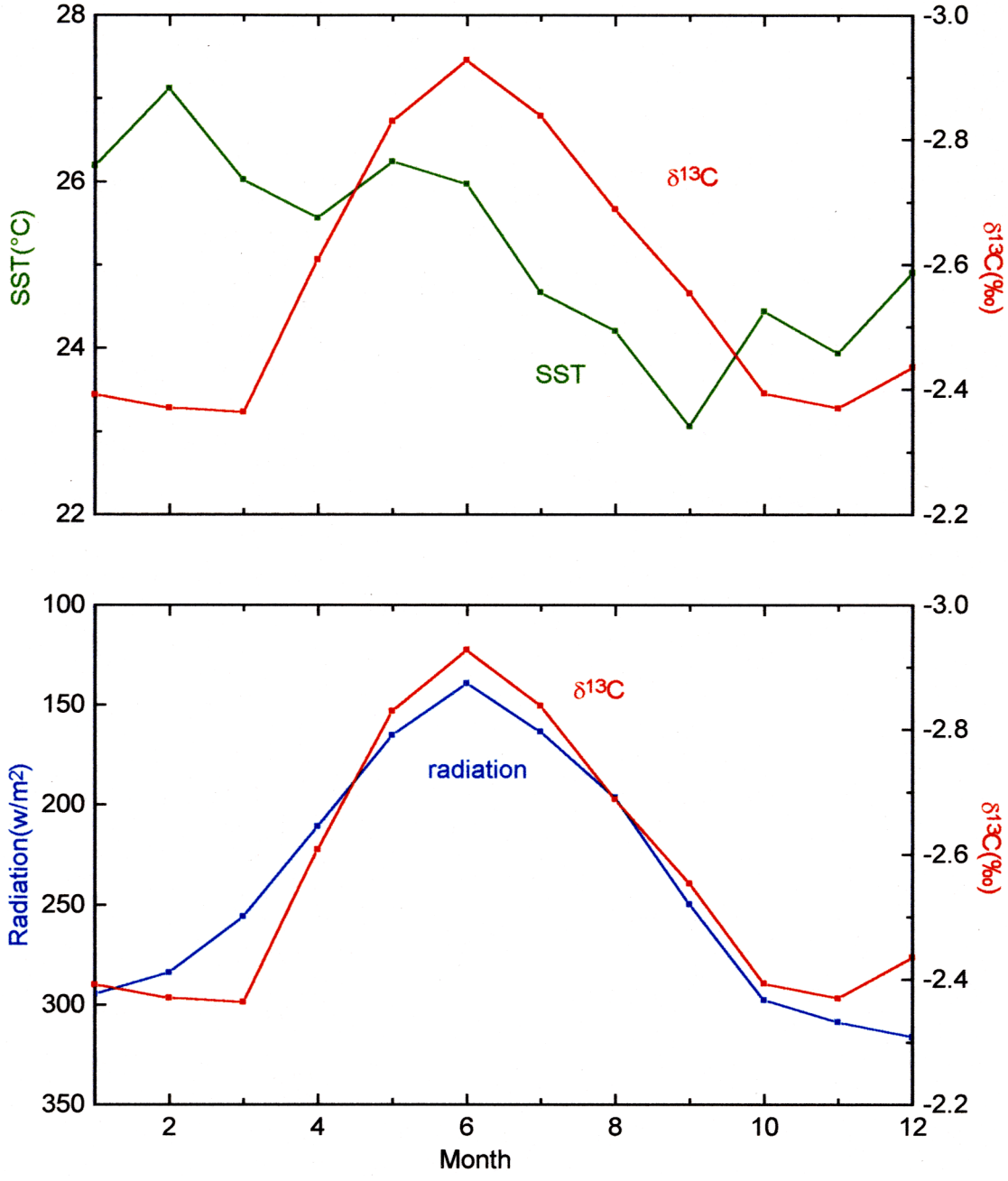

Fig. 3.4 Plots of average monthly SST (in green), solar radiation (in blue), as well as $\delta^{13}C$ in corals (in red) for Rarotonga. The SST data is from IGOSS data while solar radiation is from ISCCP and both cover the period 1983-1991. The average monthly coral $\delta^{13}C$ also covers the same period.

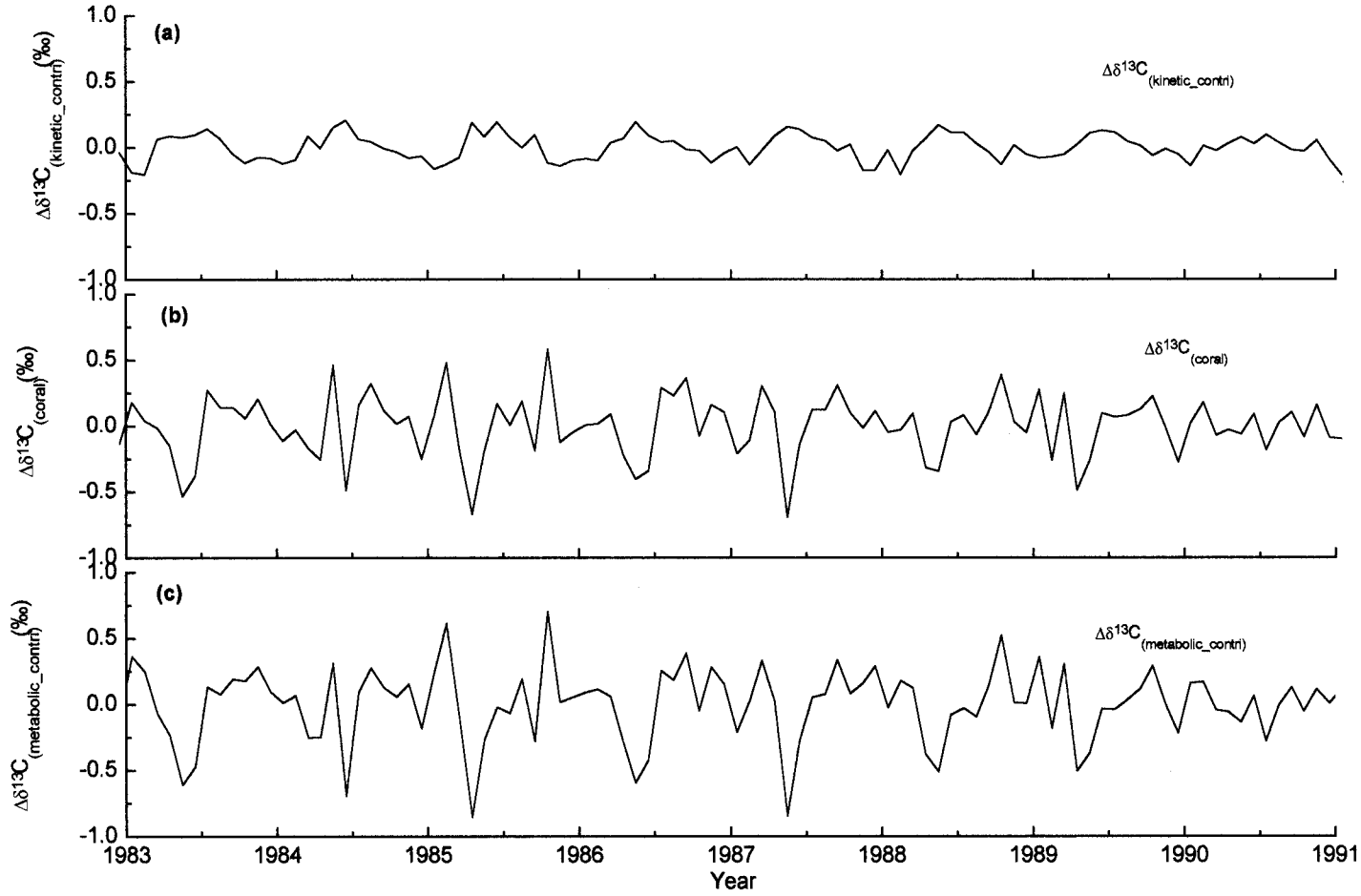

Fig. 3.5 (a) The instantaneous contribution by changes of kinetic activity to the total changes of $\delta^{13}C$ in corals for the period 1983-1991. **(b)** The instantaneous changes of $\delta^{13}C$ in corals for the period 1983-1991. **(c)** The instantaneous contribution by changes of metabolic activity to the total changes of $\delta^{13}C$ in corals for the period 1983-1991.

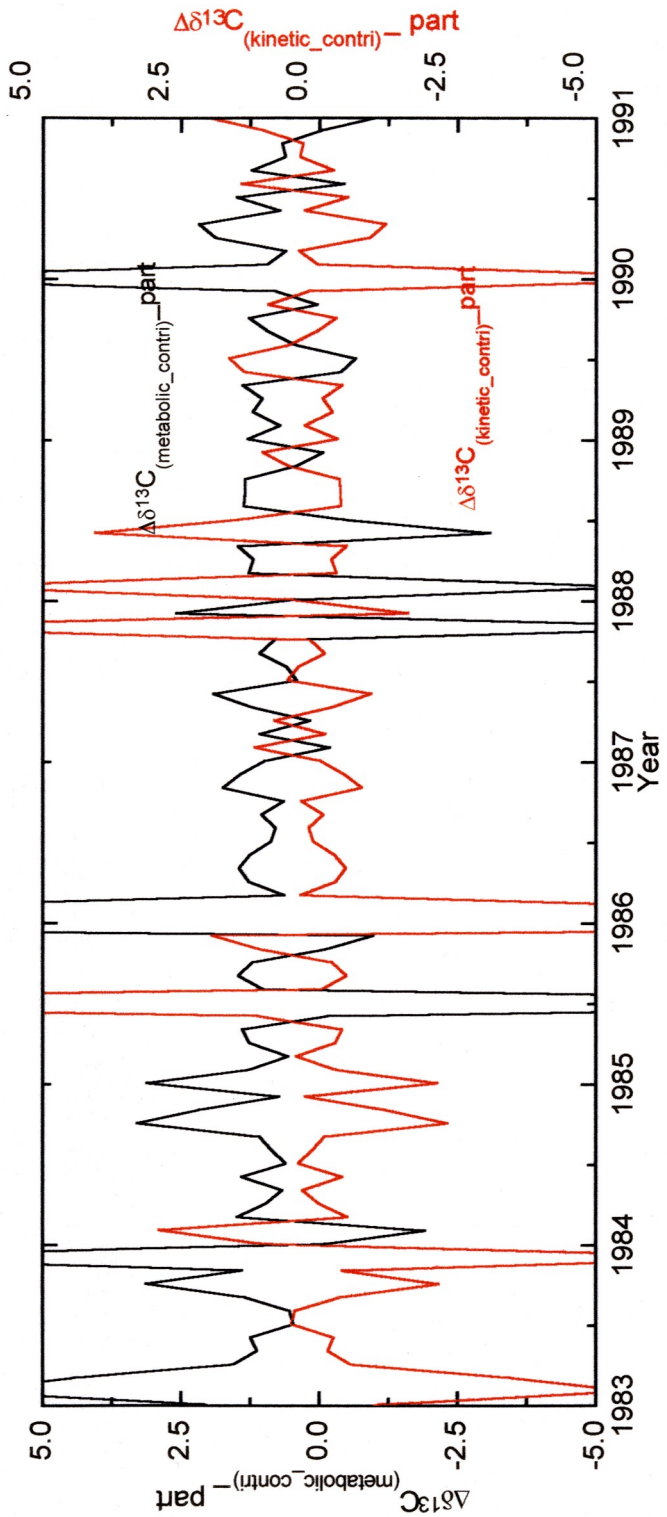

Fig. 3.6 Normalization of the two instantaneous contributions by changes of kinetic (in red) and metabolic (in black) activity to the total coral $\delta^{13}C$ changes for the period 1983-1991 to show their actual correlation with coral $\delta^{13}C$.

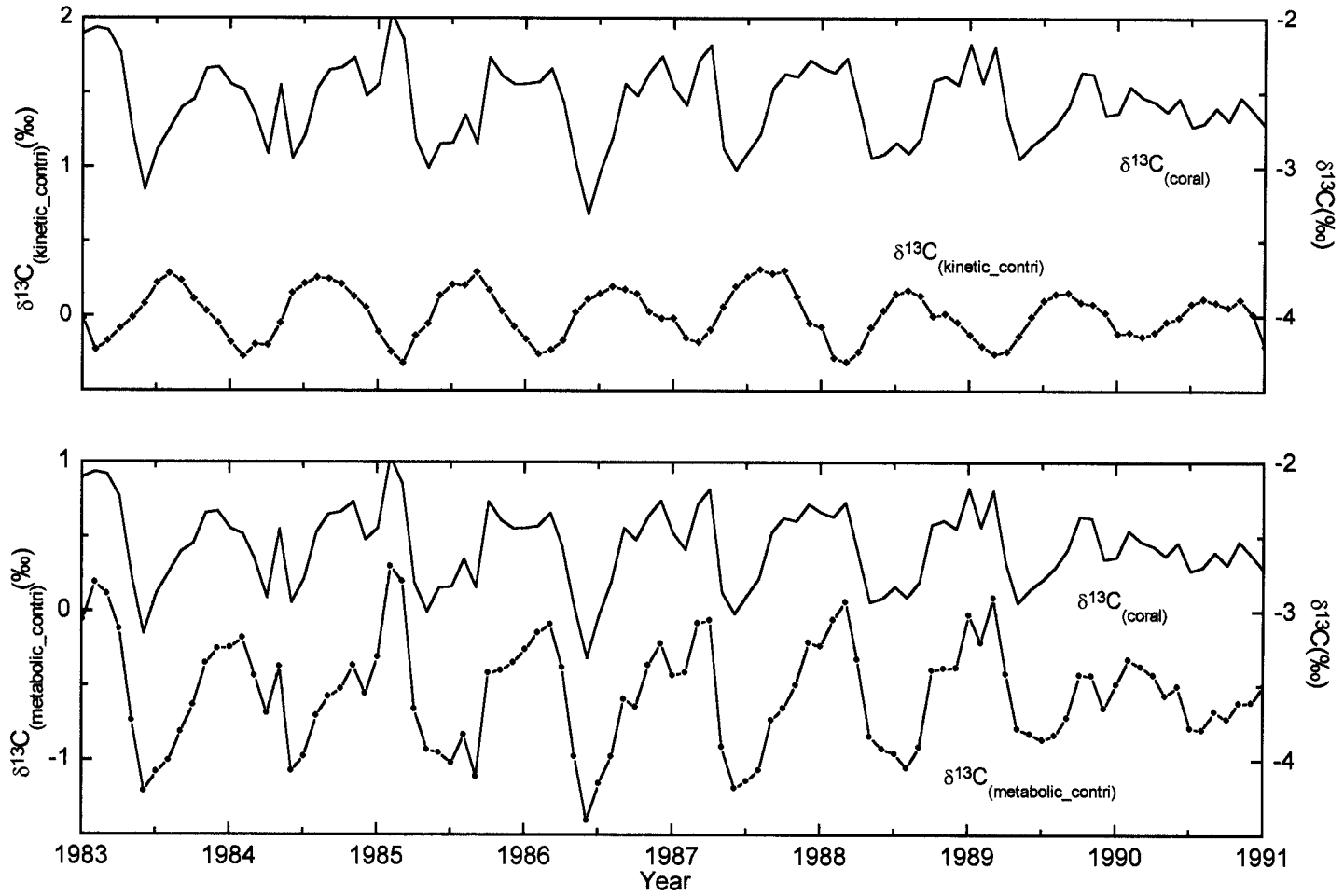

Fig. 3.7 Comparison of the accumulative contribution by changes of kinetic and metabolic activity with those of coral $\delta^{13}C$, respectively for the period 1983-1991.

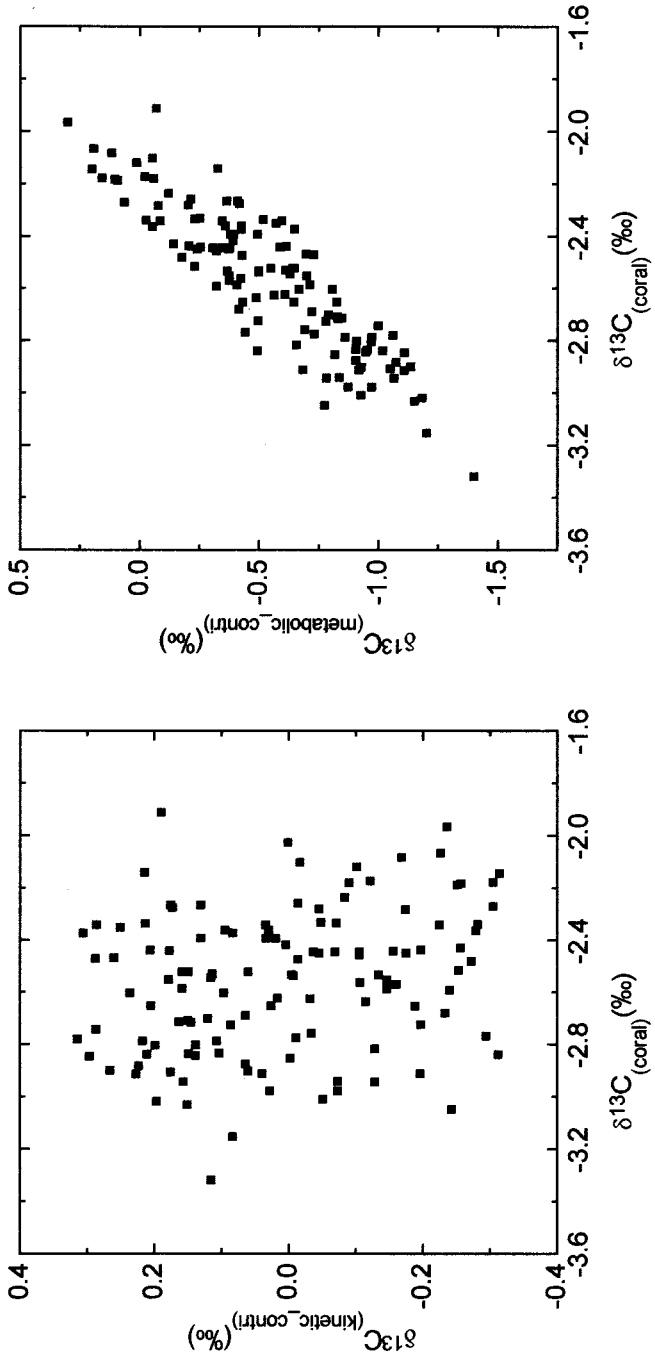

Fig. 3.8 Plots of coral $\delta^{13}C$ vs. reconstructed accumulative contributions by changes of kinetic and metabolic fractionation, respectively for the period 1983-1991.

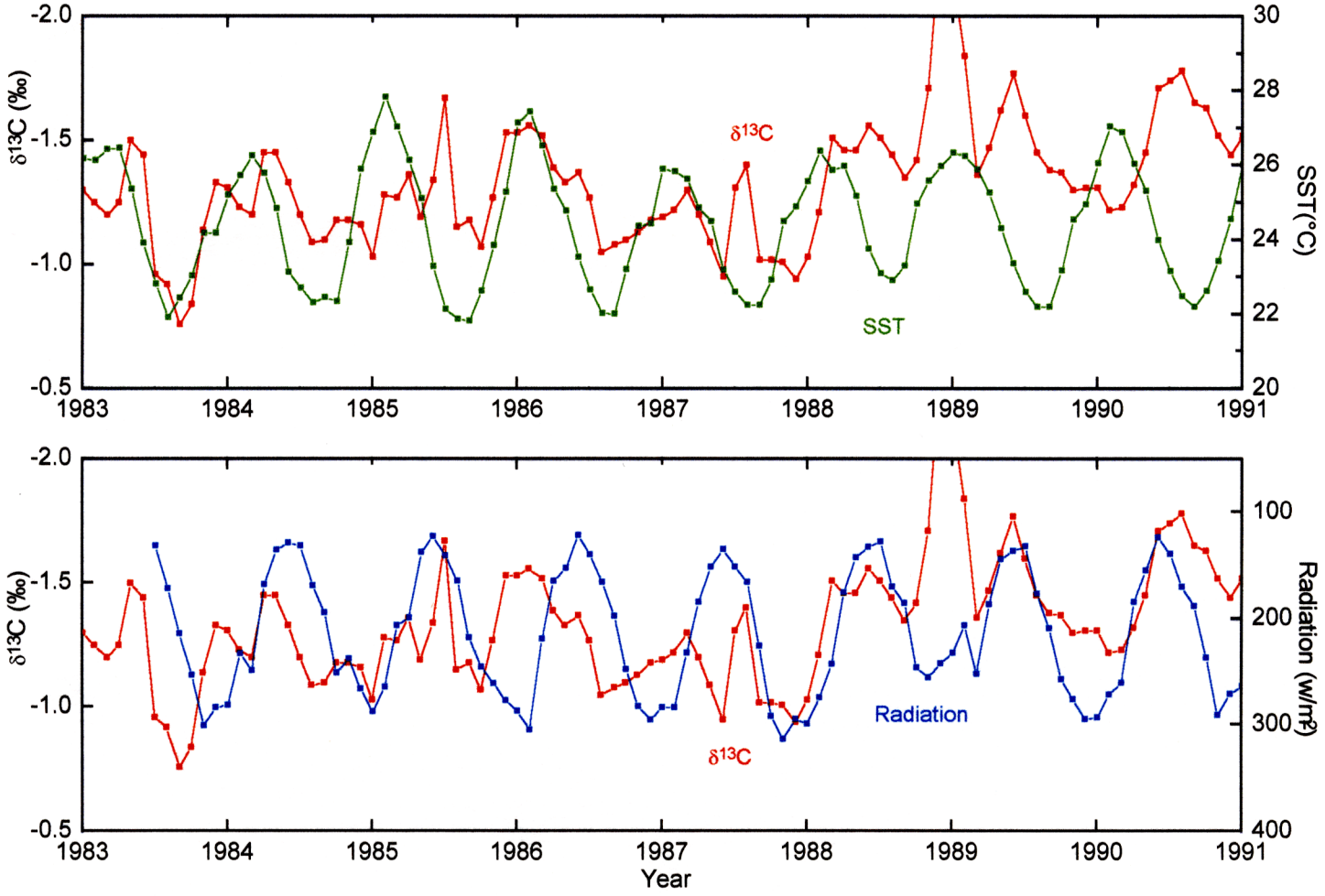

Fig. 3.9 Comparison of $\delta^{13}C$ in corals (in red) with monthly SST (in green) and solar radiation (in blue) data for the period 1983-1991 at New Caledonia. The SST data is from CAC for 2x2 degree latitude-longitude grid surrounding New Caledonia while the solar radiation data is from ISCCP for 2x2 degree latitude-longitude grid surrounding New Caledonia.

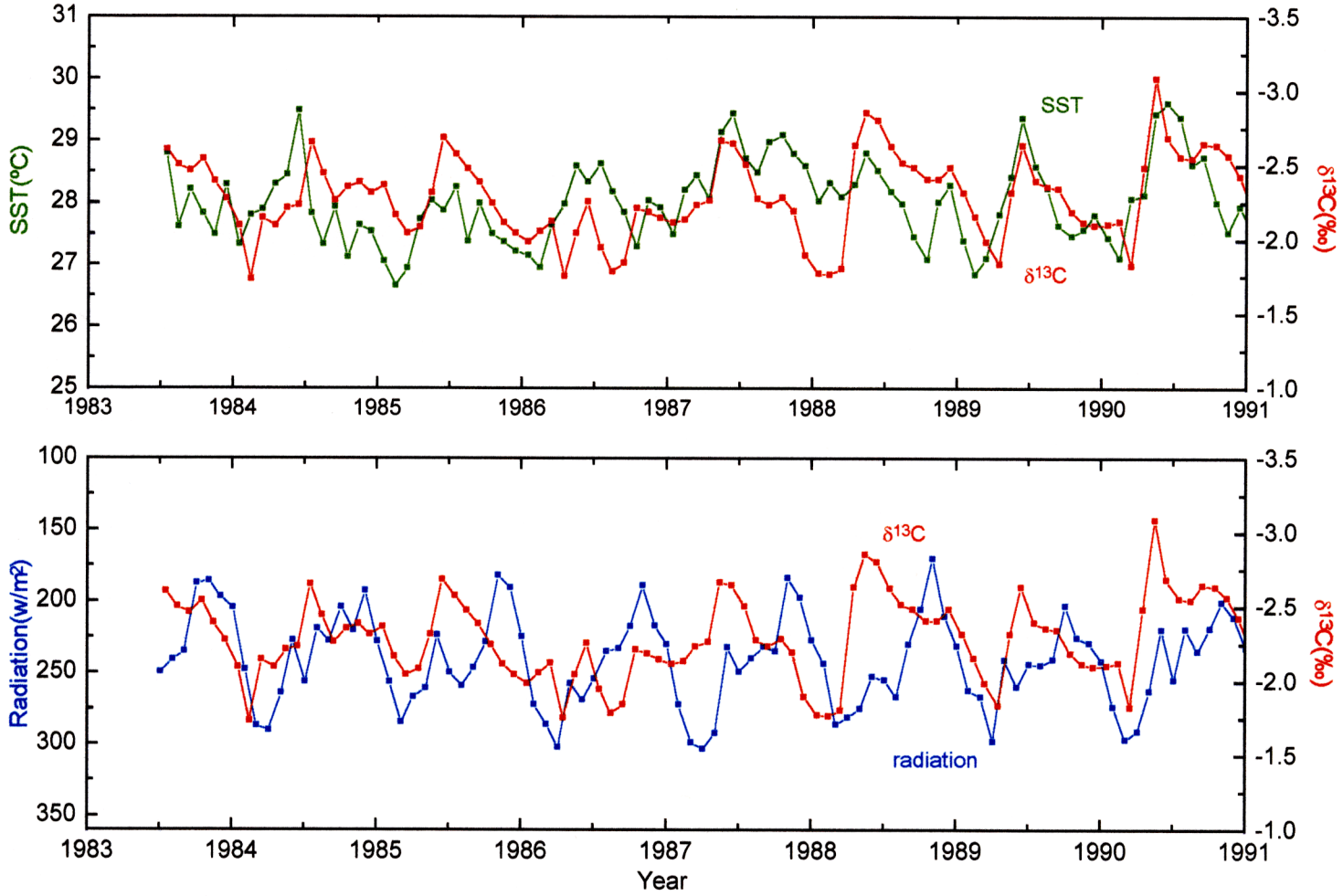

Fig. 3.10 Comparison of $\delta^{13}C$ in corals (in red) with monthly SST (in green) and solar radiation (in blue) data for the period 1983-1991 at Clipperton. The SST data is from CAC for 2x2 degree latitude-longitude grid surrounding Clipperton while the solar radiation data is from ISCCP for 2x2 degree latitude-longitude grid surrounding Clipperton.

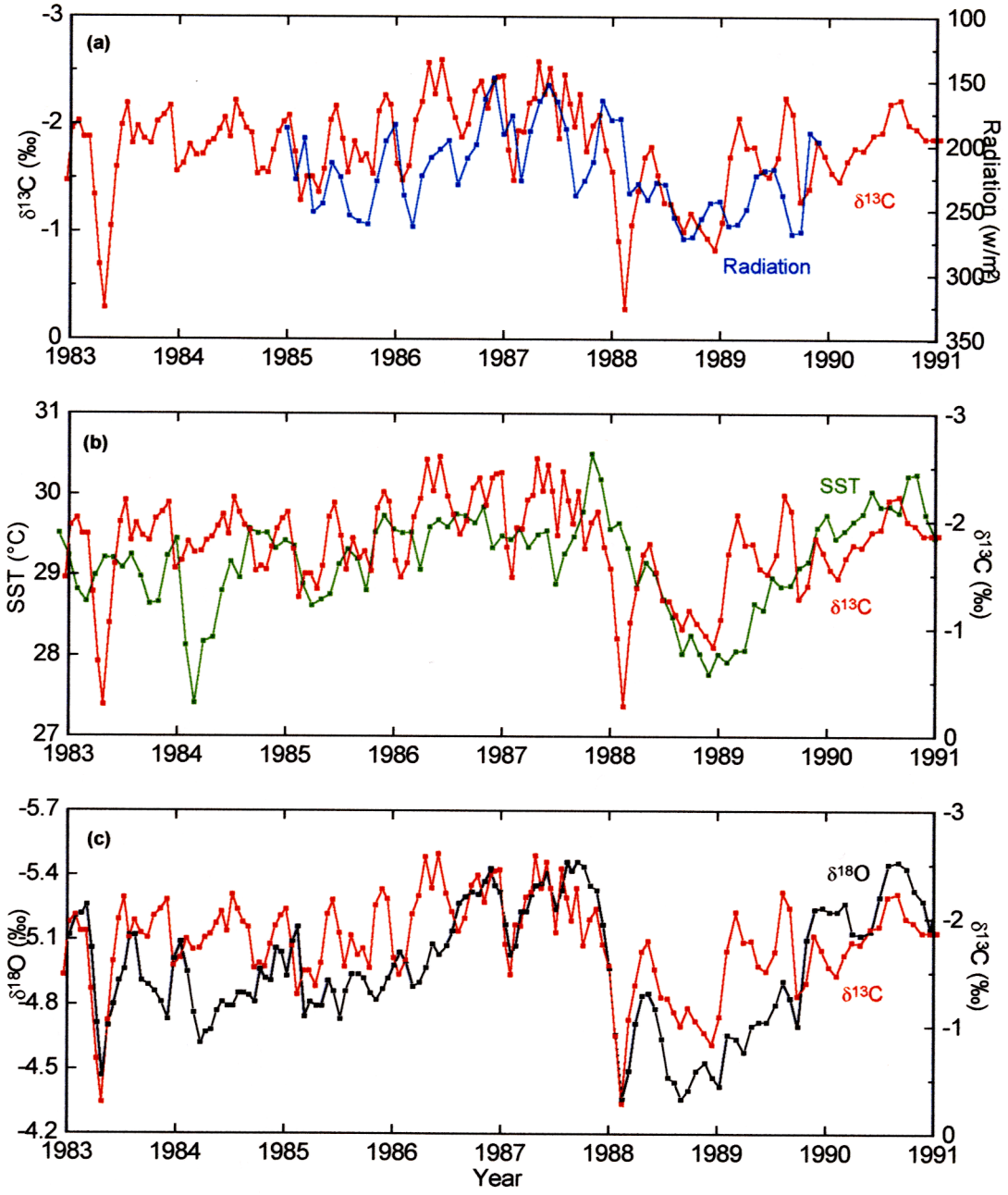

Fig. 3.11 (a) Comparison of $\delta^{13}C$ in corals (in red) with monthly solar radiation data (in blue) for the period 1983-1991 at Nauru. **(b)** Comparison of $\delta^{13}C$ in corals (in red) with monthly SST data (in green) for the period 1983-1991 at Nauru. **(c)** Comparison of $\delta^{13}C$ in corals (in red) with $\delta^{18}O$ in corals (in black) for the period 1983-1991 at Nauru. The SST data is from CAC for 2x2 degree latitude-longitude grid surrounding Nauru while the solar radiation data is from ISCCP for 2x2 degree latitude-longitude grid surrounding Nauru.

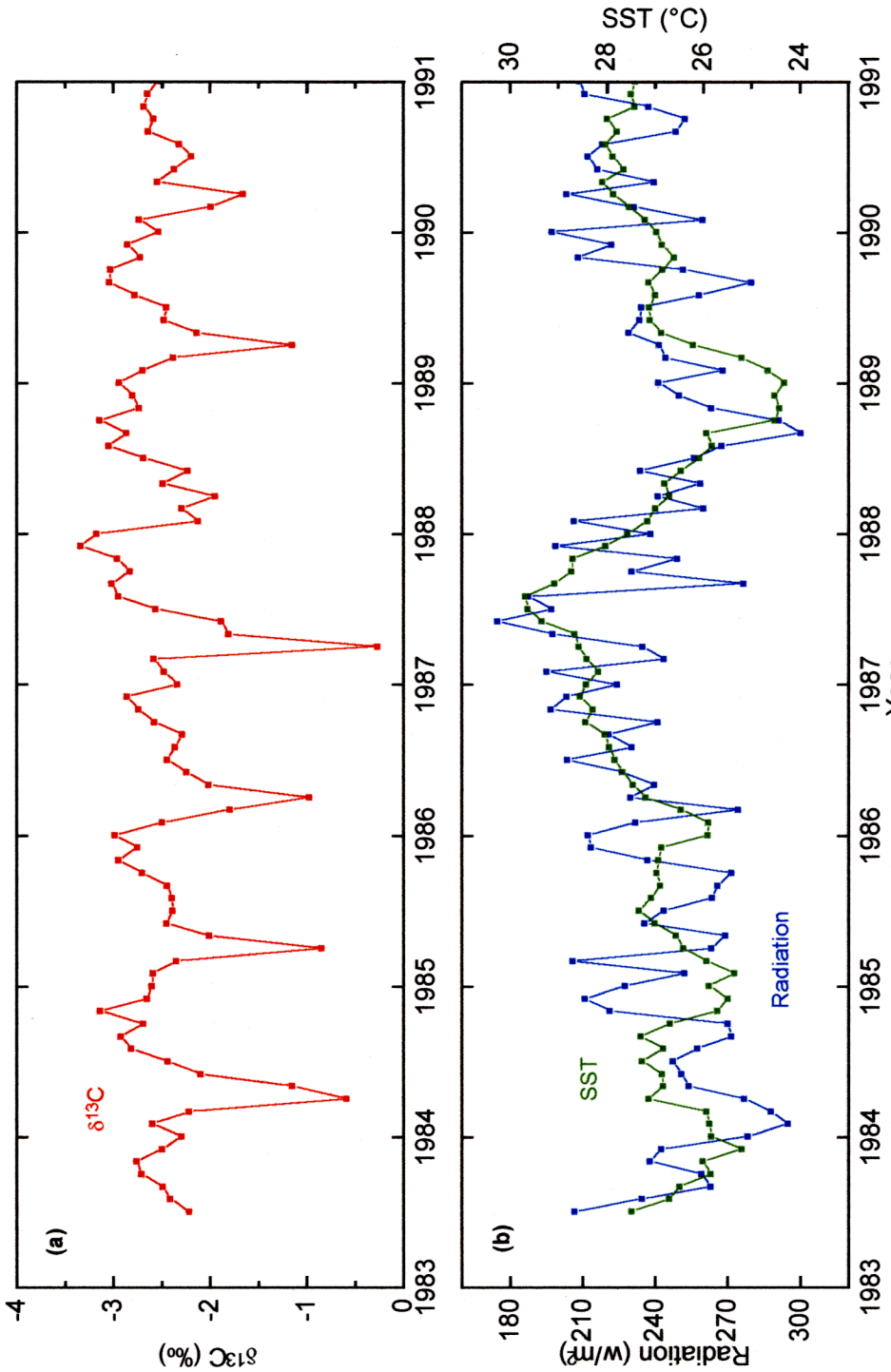

Fig. 3.12 (a) The $\delta^{13}C$ in corals (in red) for the period 1983-1991 at Kiritimati. **(b)** Comparison of monthly SST data (in green) with monthly solar radiation data (in blue) for the period 1983-1991 at Kiritimati. The SST data is from CAC for 2x2 degree latitude-longitude grid surrounding Kiritimati while the solar radiation data is from ISCCP for 2x2 degree latitude-longitude grid surrounding Kiritimati.

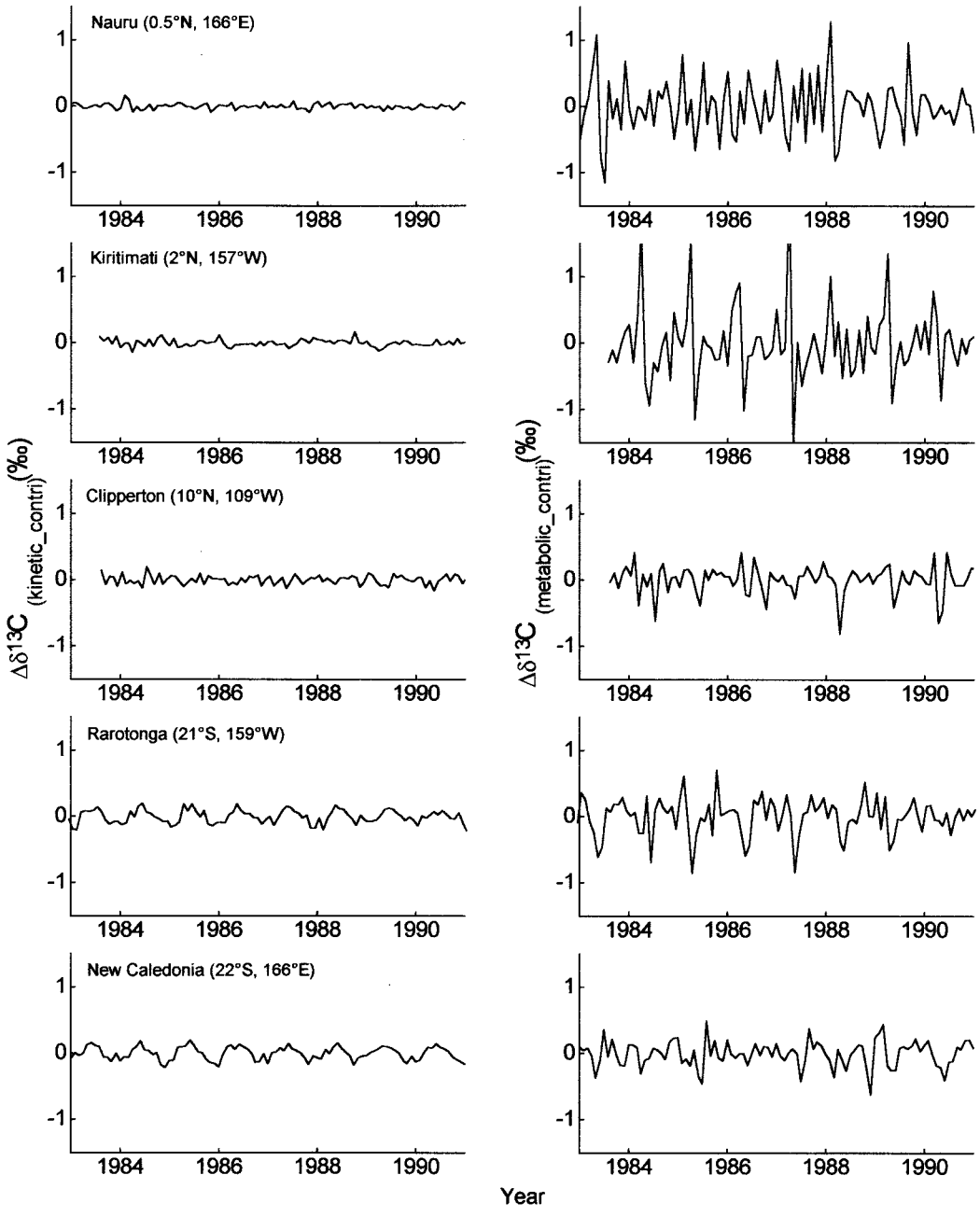

Fig. 3.13 The instantaneous contributions by changes of kinetic (left) and metabolic (right) activity to the total changes of coral $\delta^{13}C$ at Nauru, Kiritimati, Clipperton, Rarotonga, and New Caledonia, respectively for the period 1983-1991.

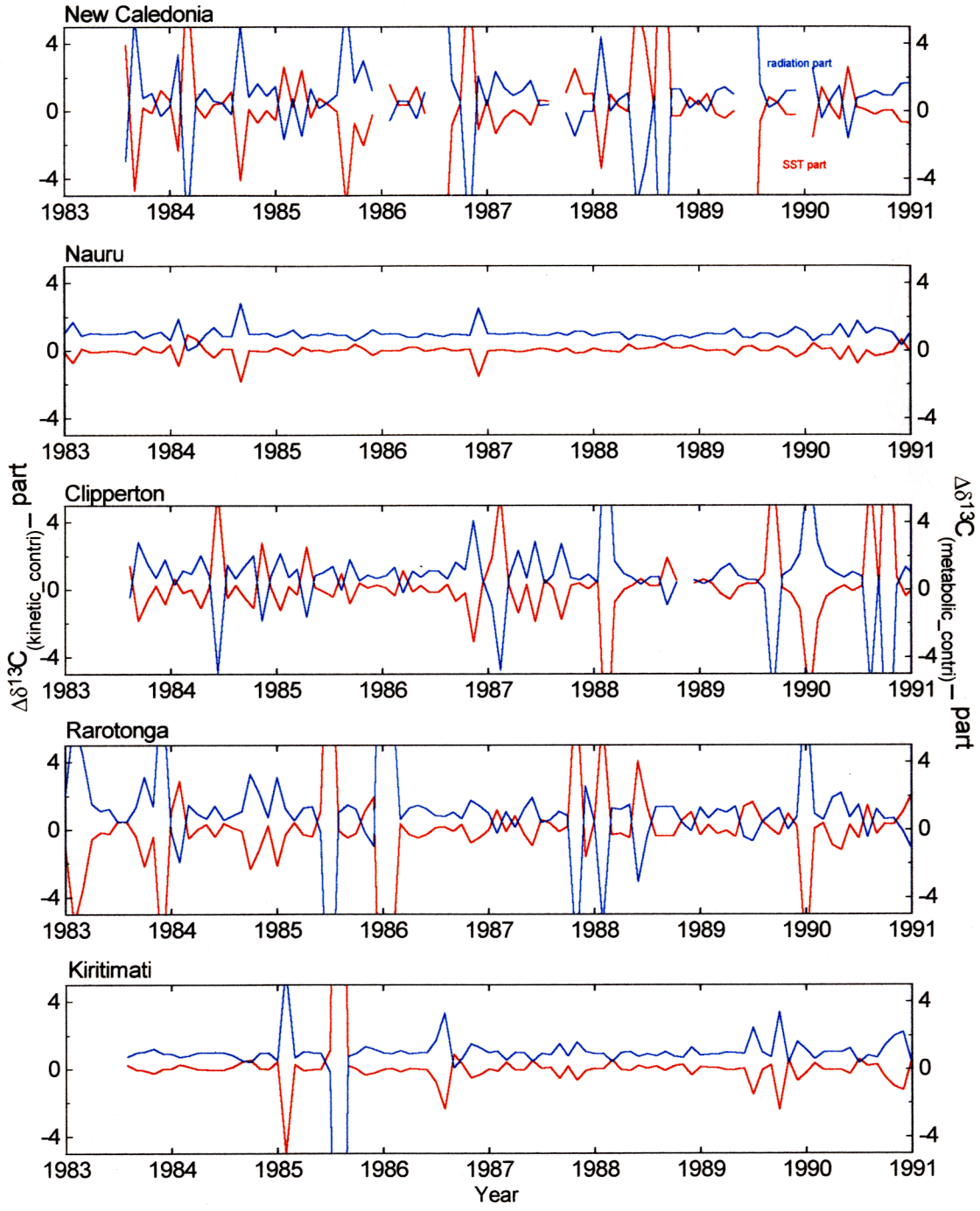

Fig. 3.14 Normalization of the two instantaneous contributions by changes of kinetic (in red) and metabolic (in blue) activity to the total coral $\delta^{13}C$ changes at Nauru, Kiritimati, Clipperton, Rarotonga, and New Caledonia, respectively for the period 1983-1991.

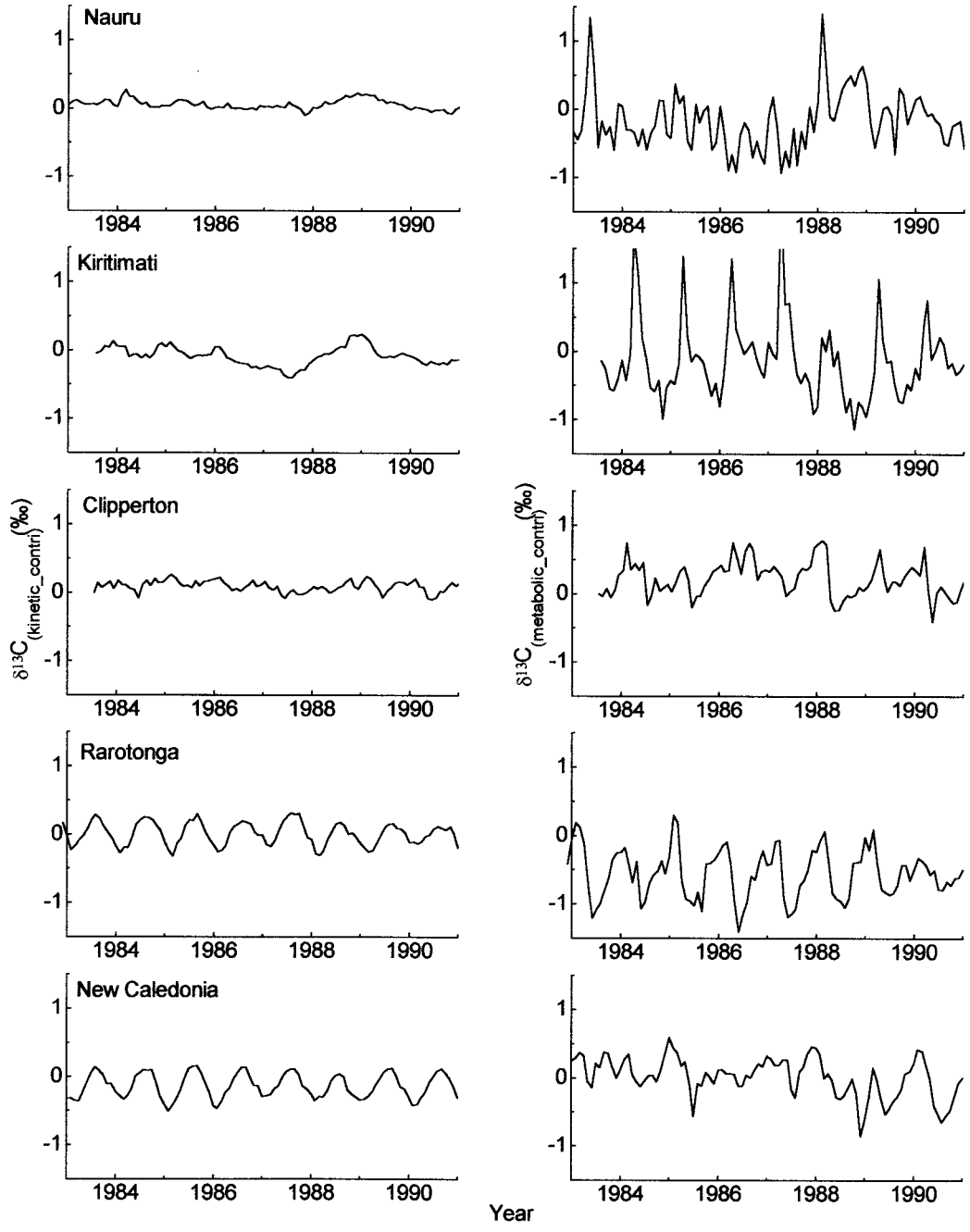

Fig. 3.15 The reconstructed accumulative contribution by changes of kinetic (left) and metabolic (right) activity to the total changes of coral $\delta^{13}C$ at Nauru, Kiritimati, Clipperton, Rarotonga, and New Caledonia, respectively for the period 1983-1991.

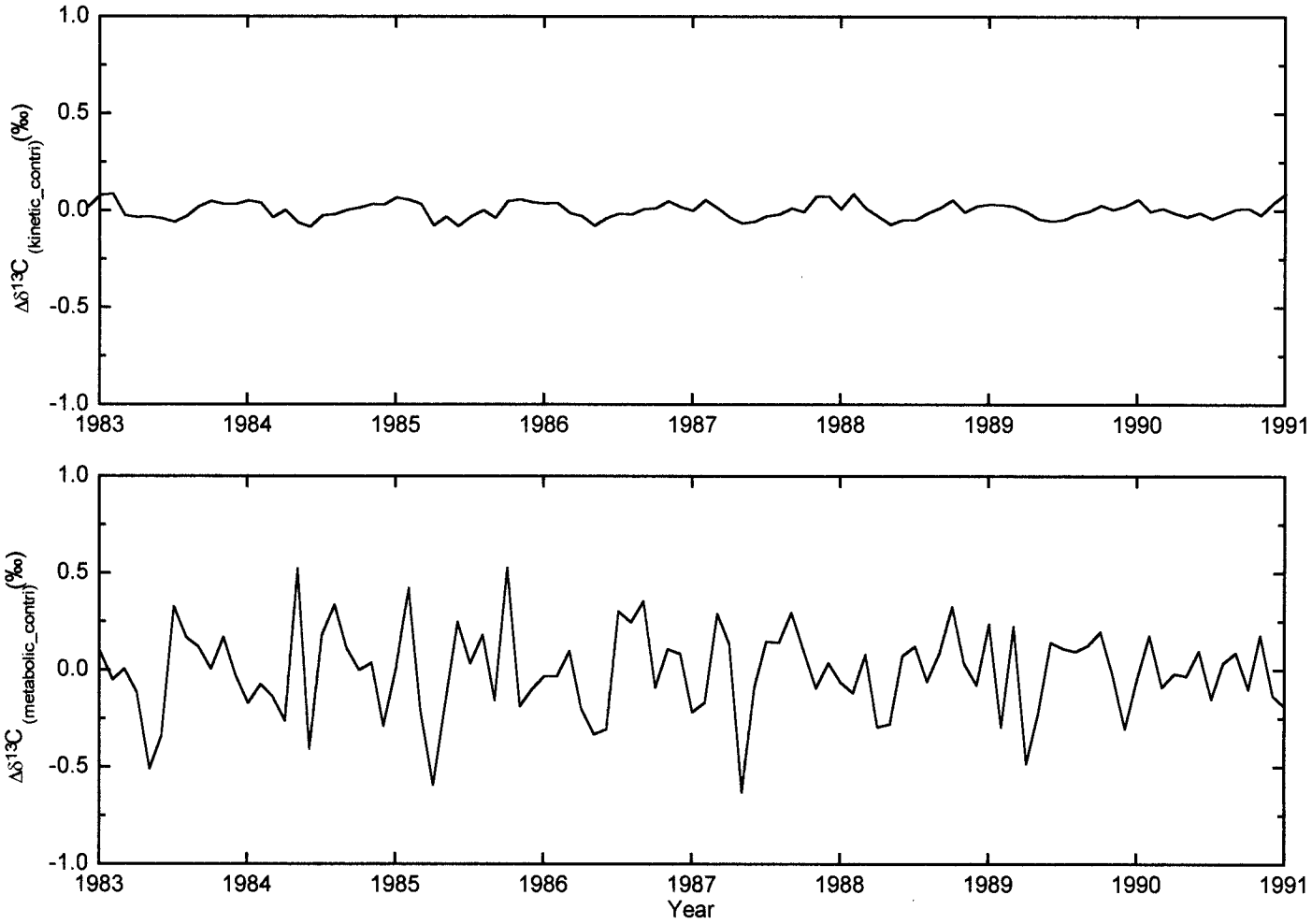

Fig. 3.16 The instantaneous contributions by changes of kinetic and metabolic activity to the total changes of $\delta^{13}C$ in corals at Rarotonga for the period 1983-1991. The partial derivative chosen for calculating the contribution of kinetic activity is 0.05‰/°C.

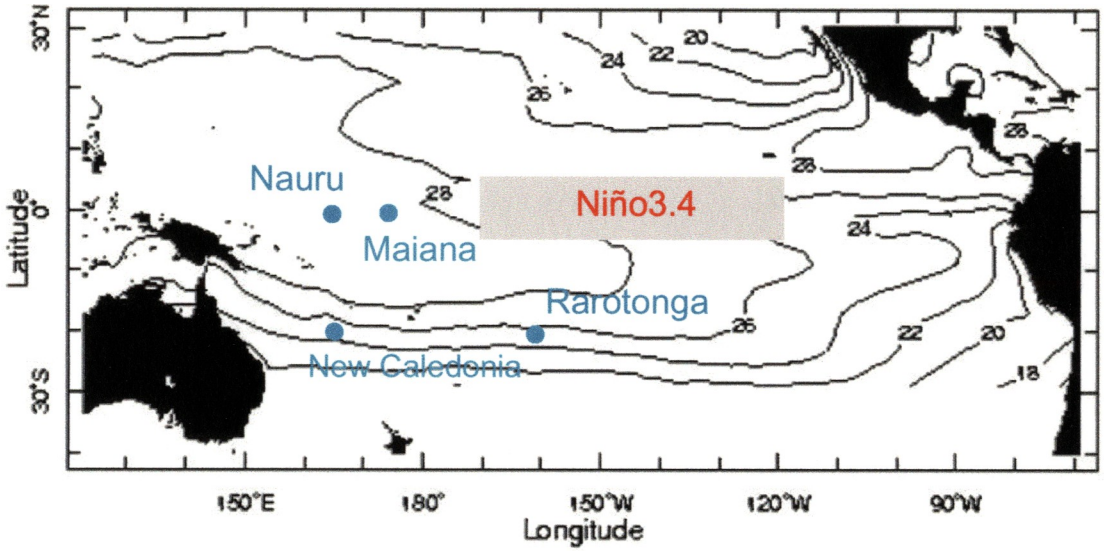

Fig. 4.1 The geographic location of Rarotonga. Also shown in the figure are the locations of New Caledonia, Nauru, and Maiana Atoll. The contours shown are sea surface temperature (SST) in the tropical Pacific in June, 2000. Also shown are the regions used to define large-scale ENSO indices: the Niño3.4 SST region is outlined by a box.

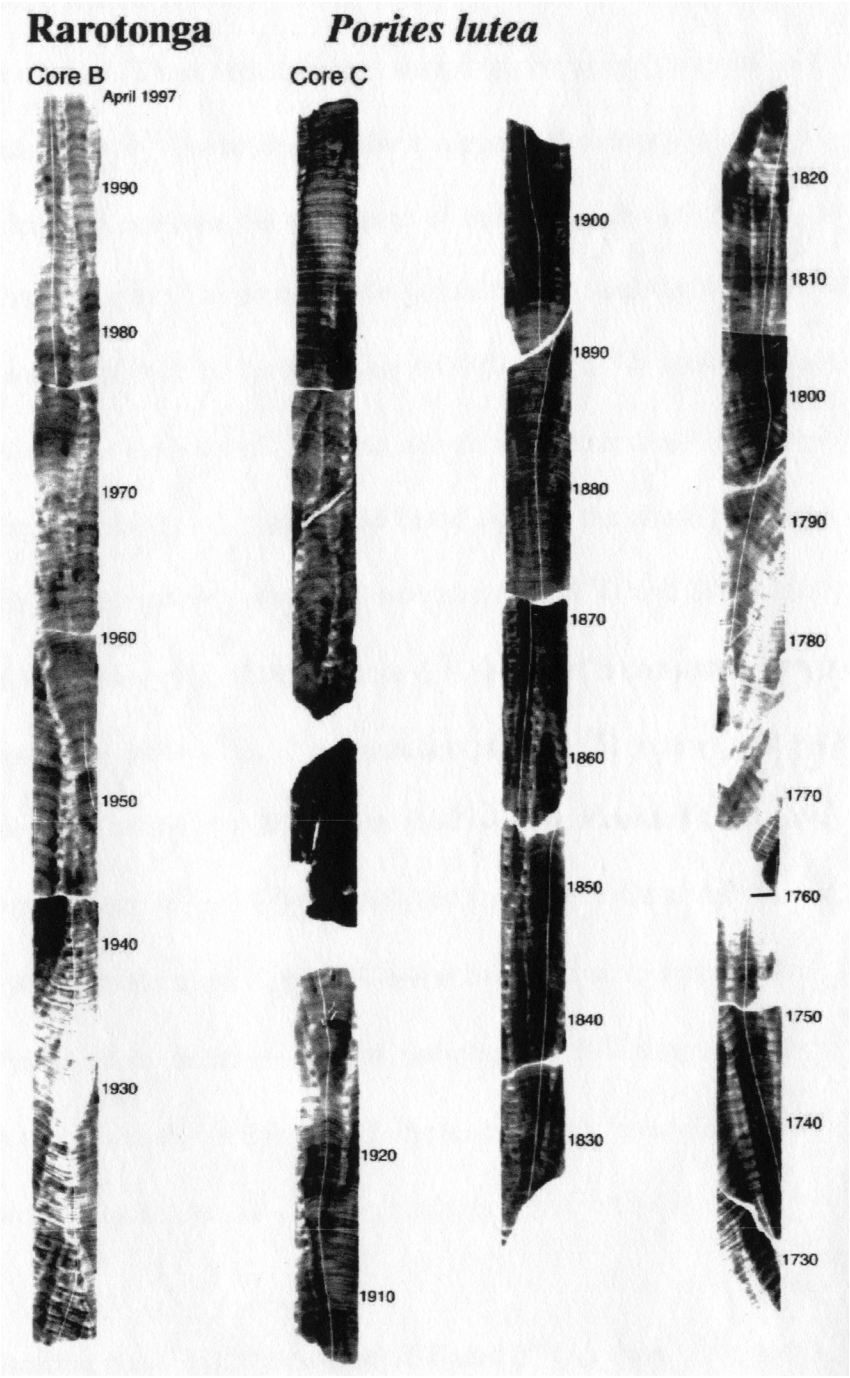

Fig. 4.2 X-ray positive collage of two coral cores (cores B and C) used in the study showing the location of mm-scale sampling transacts. Note the overall goodness of fit between the individual coral slabs except for a growth hiatus in the third section of core C.

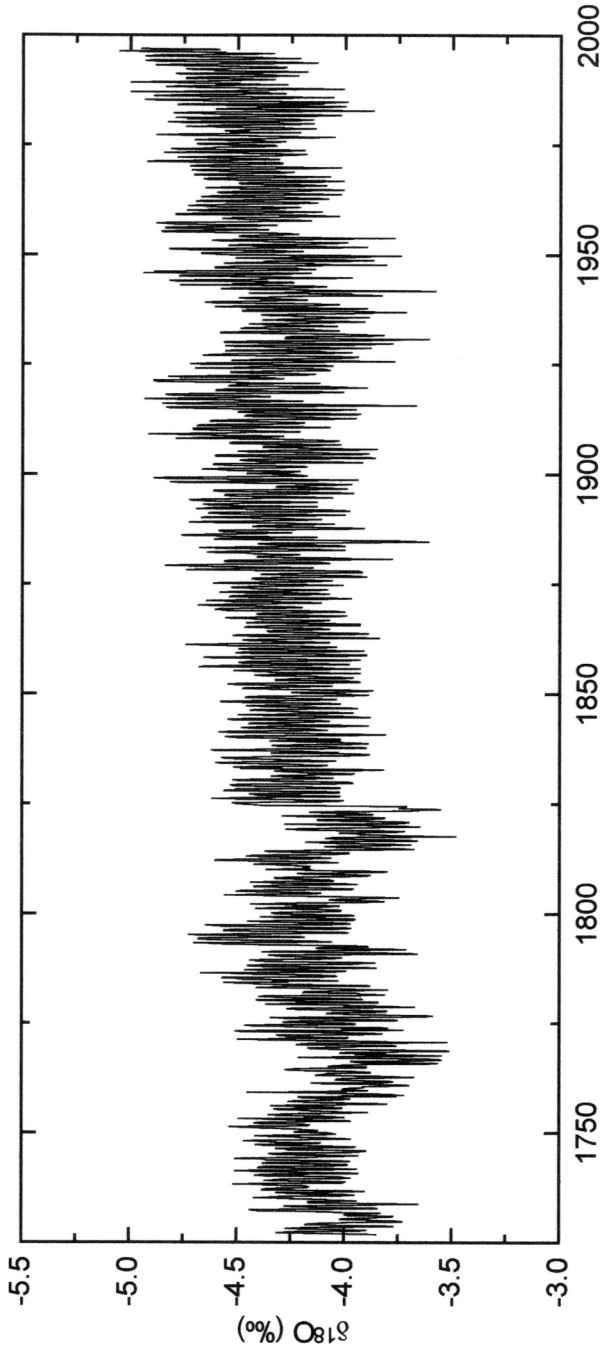

Fig. 4.3 Rarotonga subseasonal coral $\delta^{18}O$ (relative to Peedee belemnite (PDB)) spanning 1726-1997.

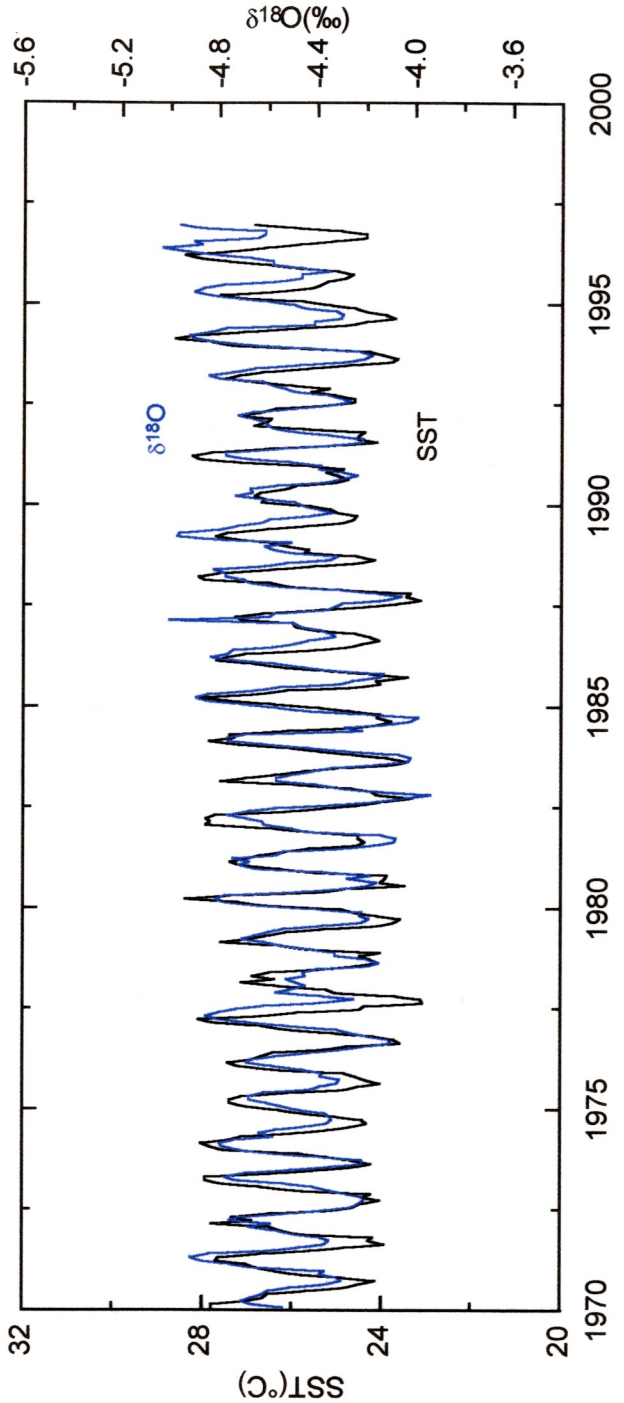

Fig. 4.4 Comparison of $\delta^{18}O$ in corals (in blue) with monthly instrumental SST data (in black) for the period 1970-1997. SST data is from CAC-NMC data archive for the 2x2 degree latitude-longitude block surrounding Rarotonga.

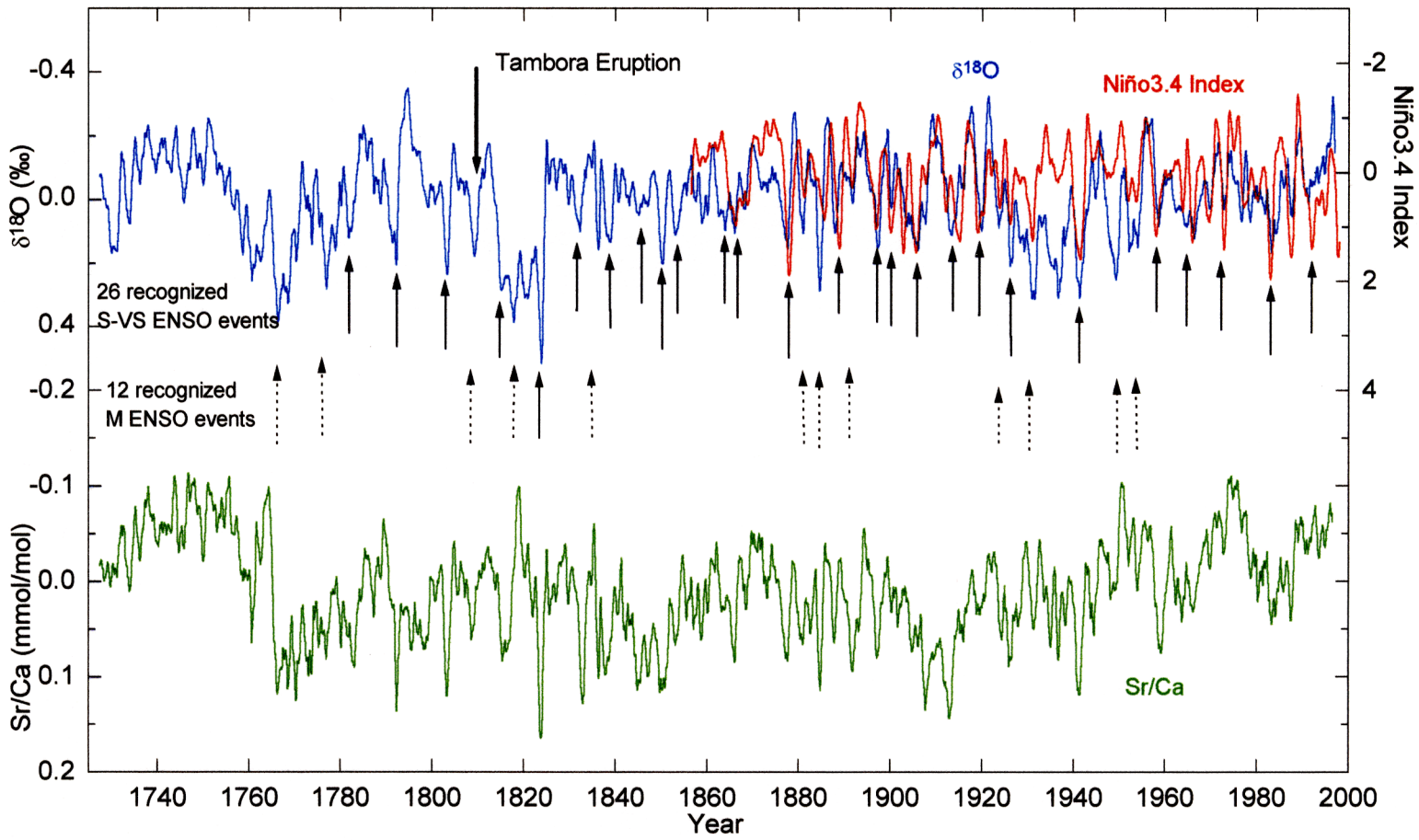

Fig. 4.5 Comparison of annual averaged record of coral $\delta^{18}O$ (in blue) from Rarotonga with annual averaged Niño3.4 Index (in red) for the period 1726-1997. The black arrows represent the strong and very strong ENSO events reconstructed by Quinn (1987; 1992) while the dotted black arrows represent the moderate ENSO events reconstructed by Quinn (1987; 1992). The annual averaged record of coral Sr/Ca (in green) is also shown. All curves are detrended and 1-year smoothing to emphasize the interannual variability.

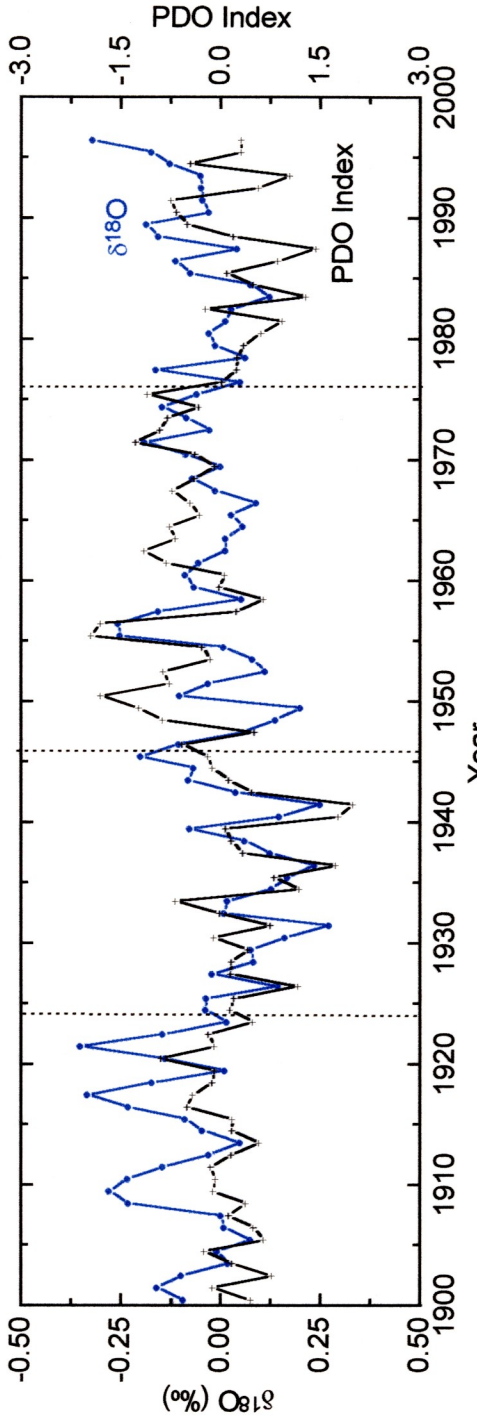

Fig. 4.6 Comparison of annually average Rarotonga coral $\delta^{18}O$ and annually averaged PDO Index for the period of 1900-1997. The dashed black lines represent the stages of decadal variability recognized in the PDO (Mantua et al., 1997).

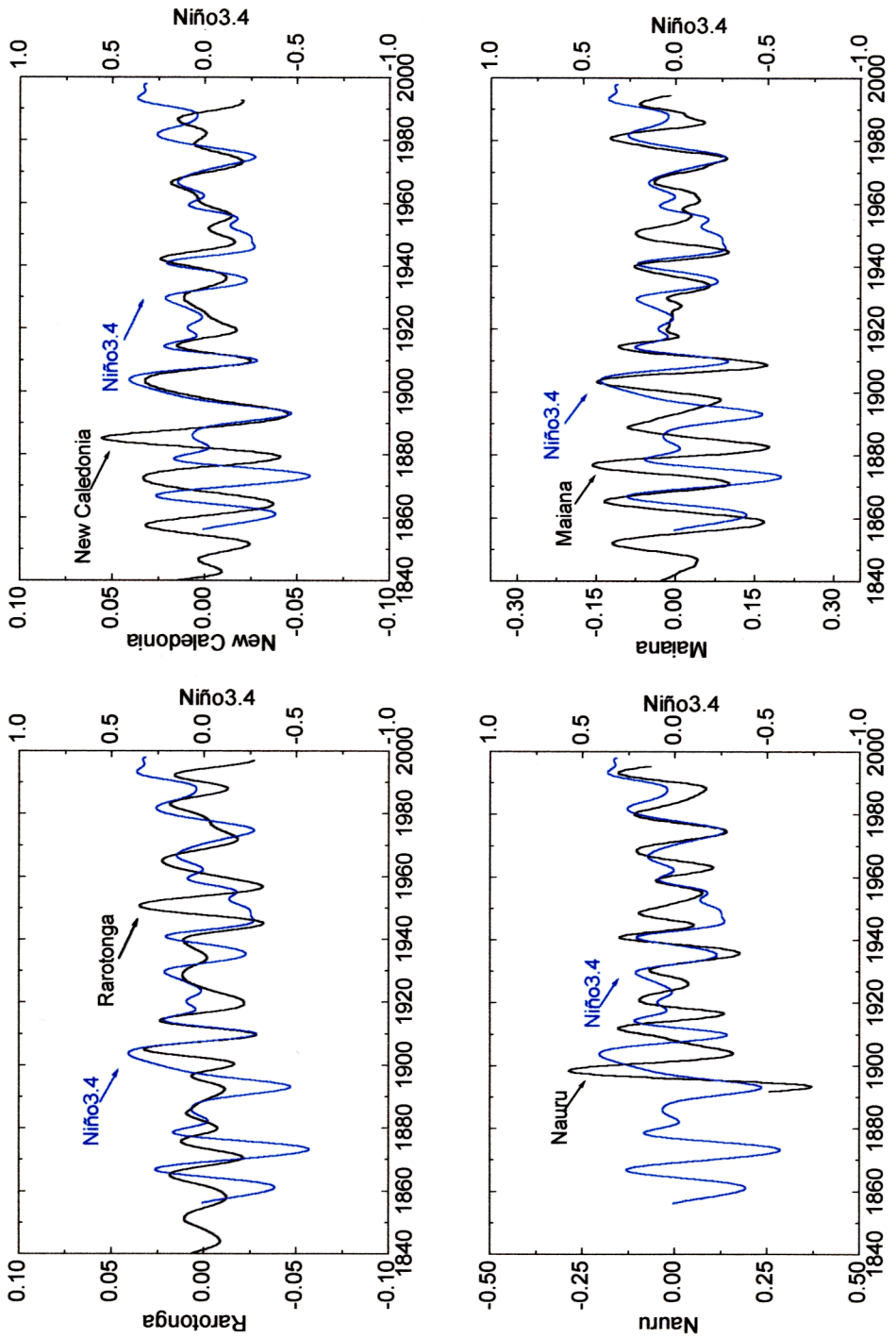

Fig. 4.7 Comparison of singular spectrum analysis (SSA) extracted decadal band RCs from Rarotonga, New Caledonia, Nauru and Maiana Atoll (in black) with that of Niño3.4 Index (in blue) for the period 1840-1997. Note that the scales of Niño3.4 Index are the same for the four regions while the scales of decadal band of coral $\delta^{18}O$ are different.

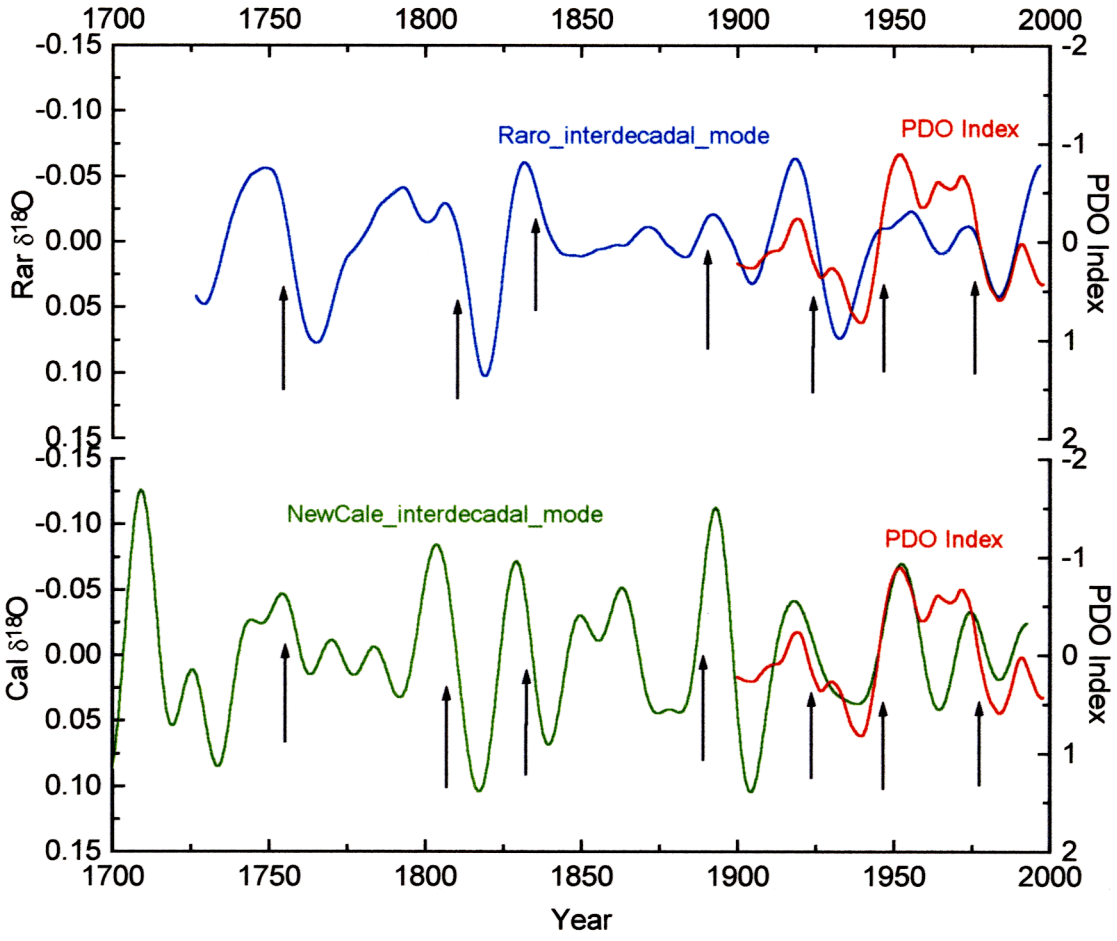

Fig. 4.8 Comparison of singular spectrum anlaysis (SSA) extracted interdecadal band RCs of $\delta^{18}O$ from Rarotonga (in blue), and New Caledonia (in green) with that of PDO Index (in red) for the period 1900-1997. Comparison of SSA extracted interdecadal bands RCs of $\delta^{18}O$ from Rarotonga and New Caledonia in the period 1700-1997. The black arrows represent the correlation observed between $\delta^{18}O$ in Rarotonga and that in New Caledonia.

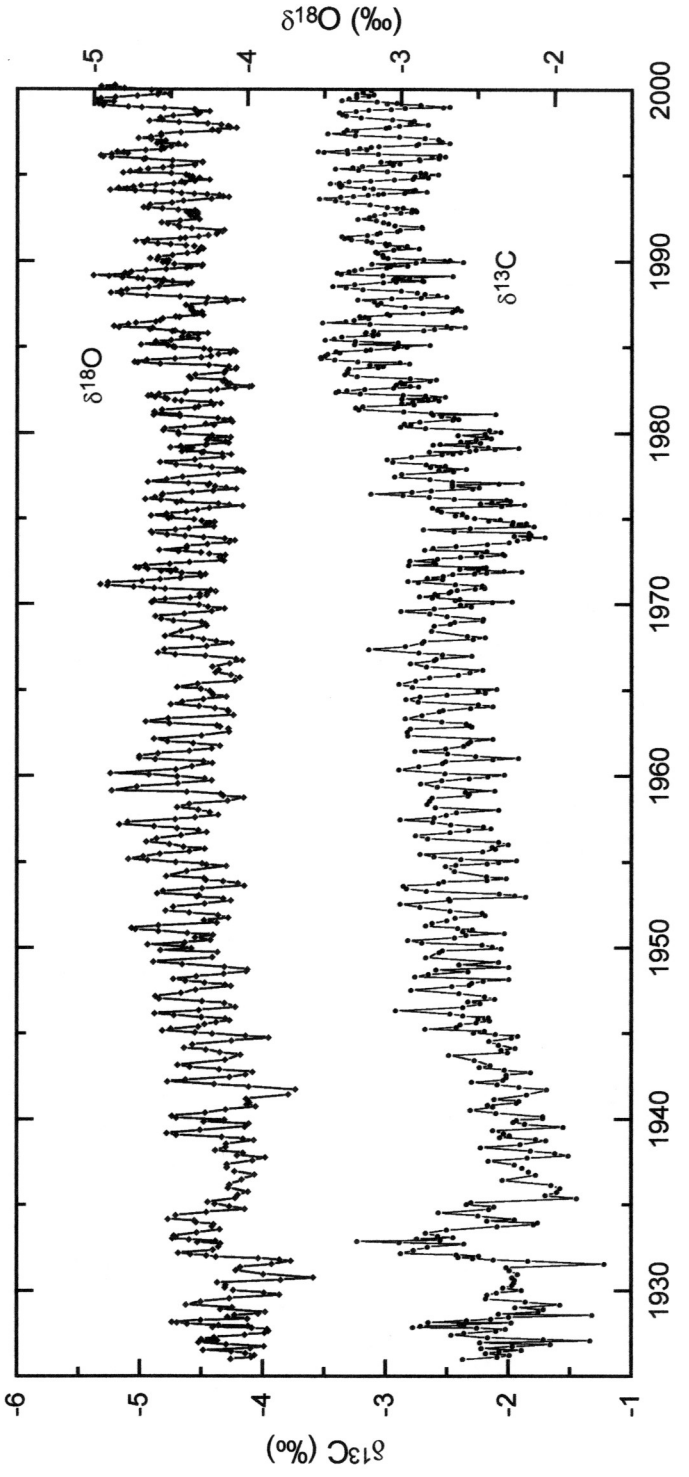

Fig. 5.1 Rarotonga subseasonal $\delta^{18}O$ and $\delta^{13}C$ of core 3R spanning the period 1926-2000.

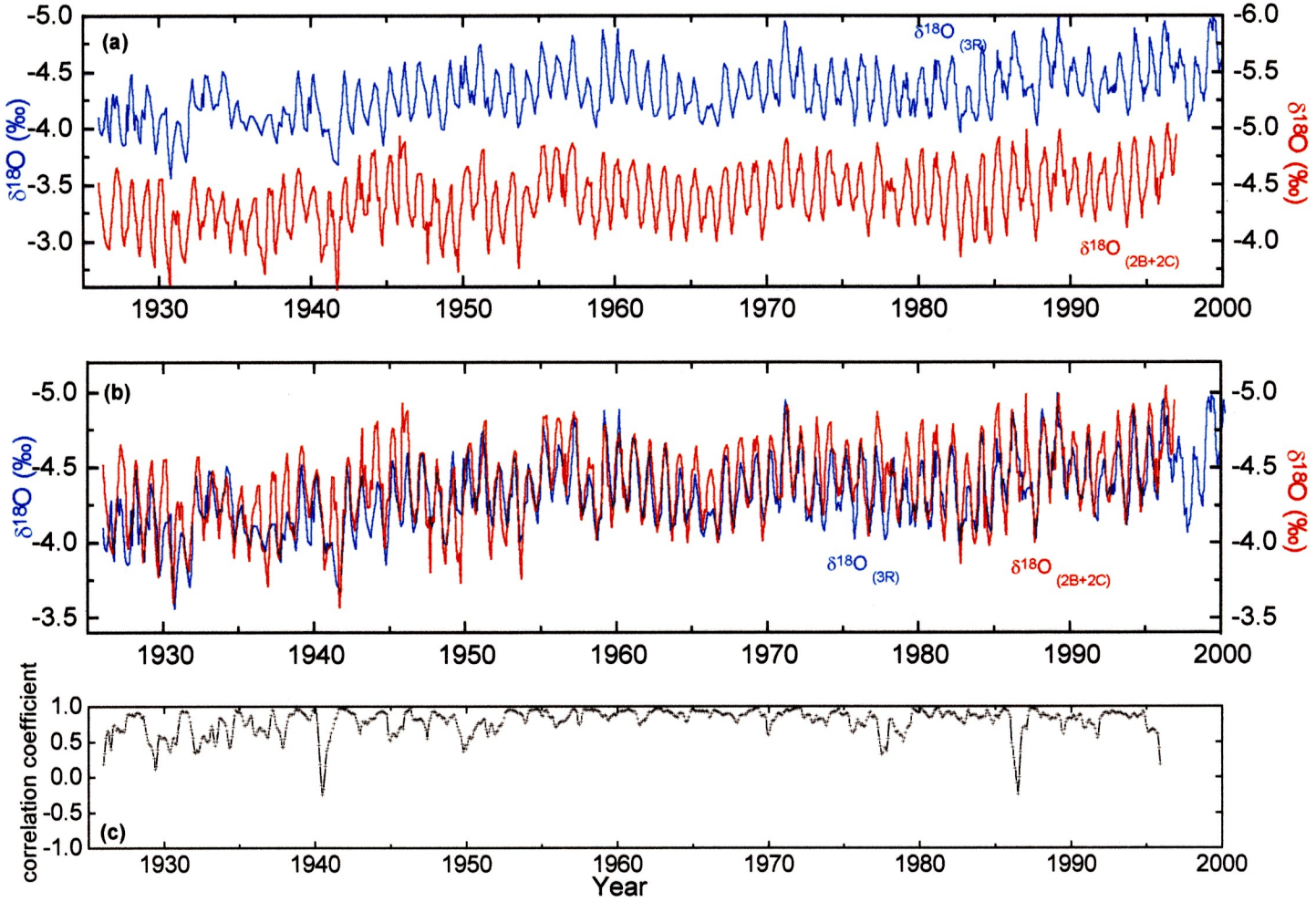

Fig. 5.2 (a) & (b) Comparison of $\delta^{18}O$ of core 2B+2C (in red) with that of core 3R (in blue) for the period 1926-1997 at Rarotonga. **(c)** Moving correlation coefficient (1-year window) showing the correlation between 2B+2C and 3R $\delta^{18}O$.

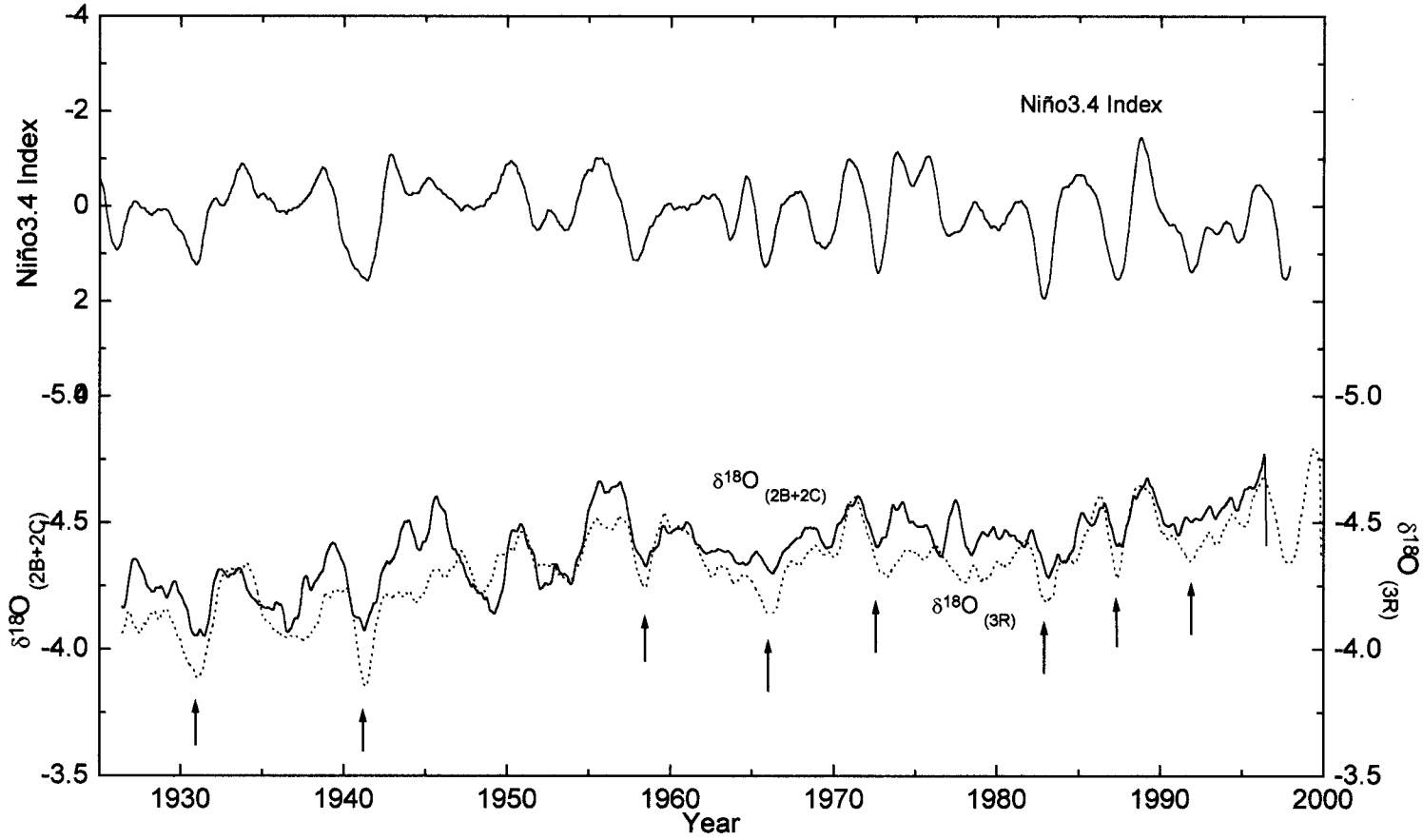

Fig. 5.3 Comparison of 12-month running average record of 2B+2C coral $\delta^{18}O$ (in solid line) with 3R coral $\delta^{18}O$ (in dotted line) from Rarotonga for the period 1926-1997. The black arrows represent the strong and very strong ENSO events reconstructed by Quinn (1987; 1992). The 12-month running average record of Niño3.4 SST Index is also shown.

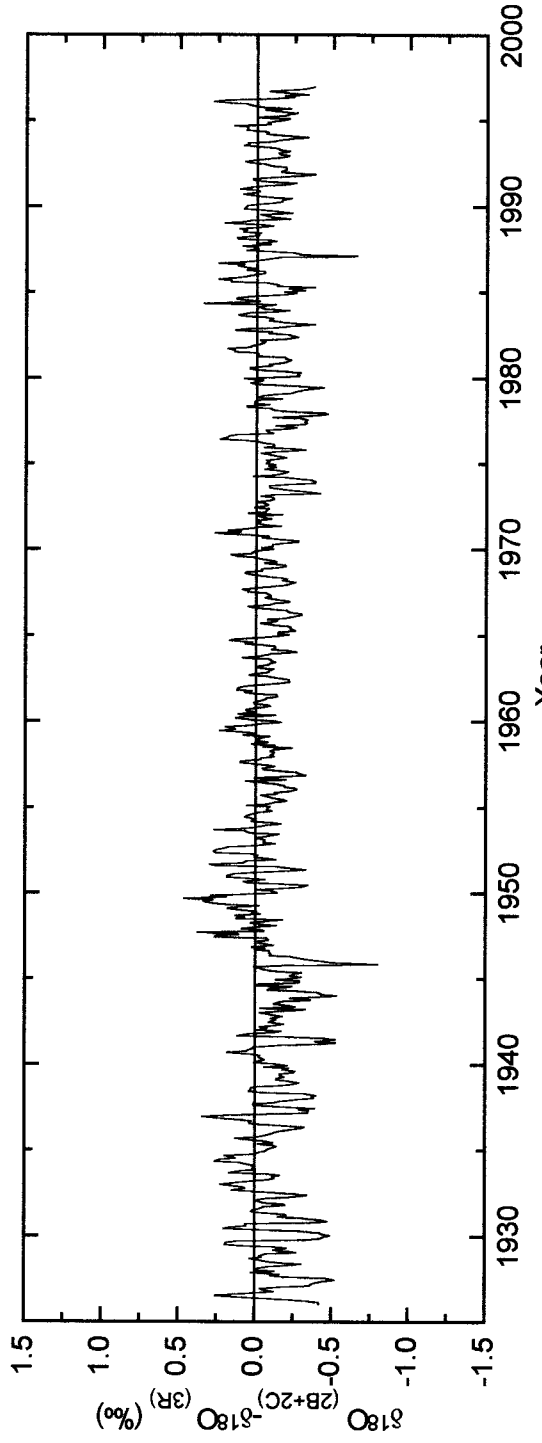

Fig. 5.4 The differences in $\delta^{18}O$ between the record 2B+2C and 3R ($\delta^{18}O_{2B+2C} - \delta^{18}O_{3R}$) for the period 1926-1997 at Rarotonga.

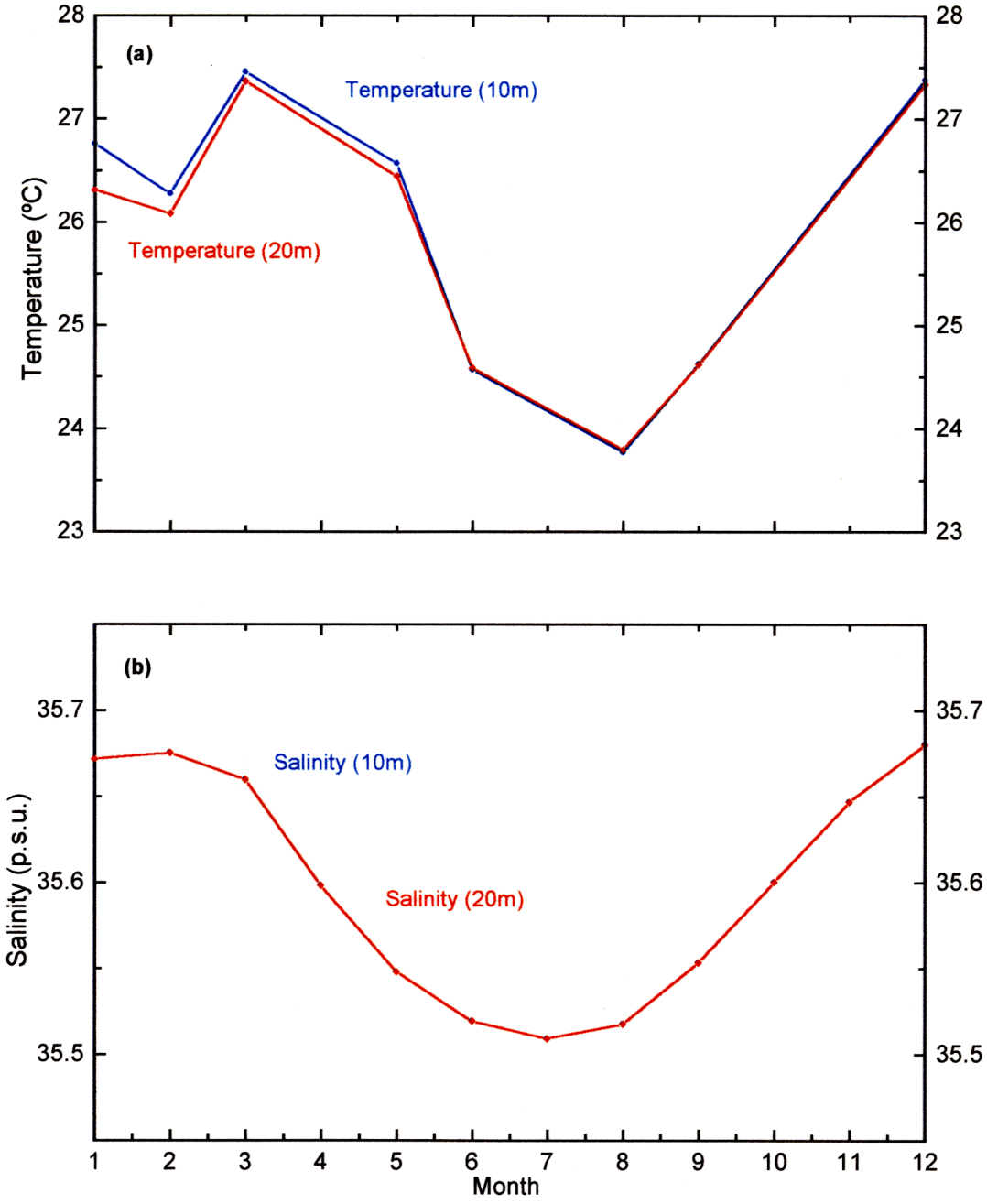

Fig. 5.5 (a) Monthly average seawater temperature at 10m (in blue) and 20m (in red) at Rarotonga (NOAA NODC WOA 98 monthly temperature) (Conkright et al., 1998). **(b)** Monthly average salinity at 10m (in blue) and 20m (in red) at Rarotonga (NOAA NCEP EMC CMB Pacific monthly salinity) (Ji et al., 1995).

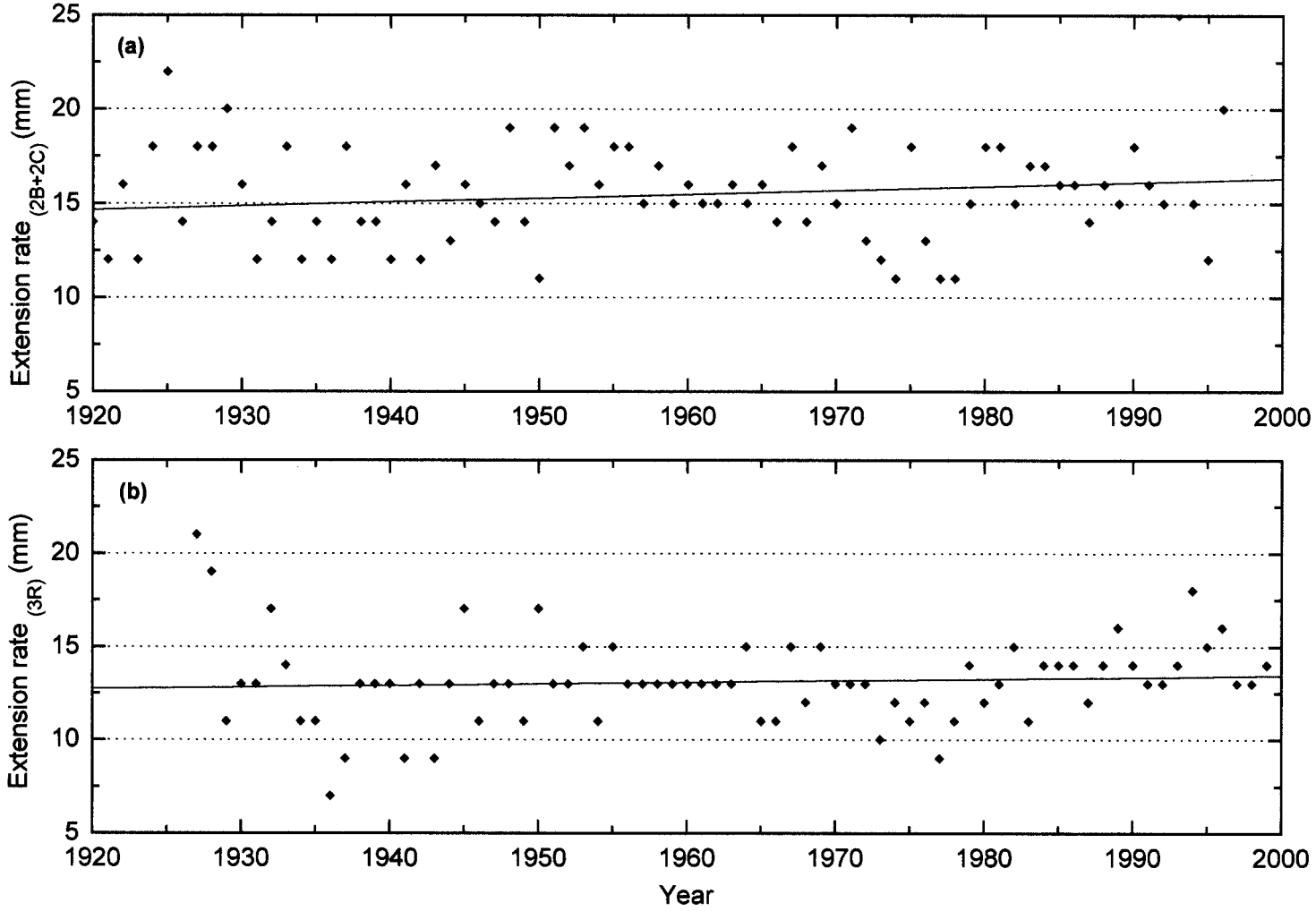

Fig. 5.6 The extension rates of **(a)** core 2B+2C and **(b)** 3R for the period 1926-2000, respectively at Rarotonga. The line in each figure represents the trend of each extension rate.

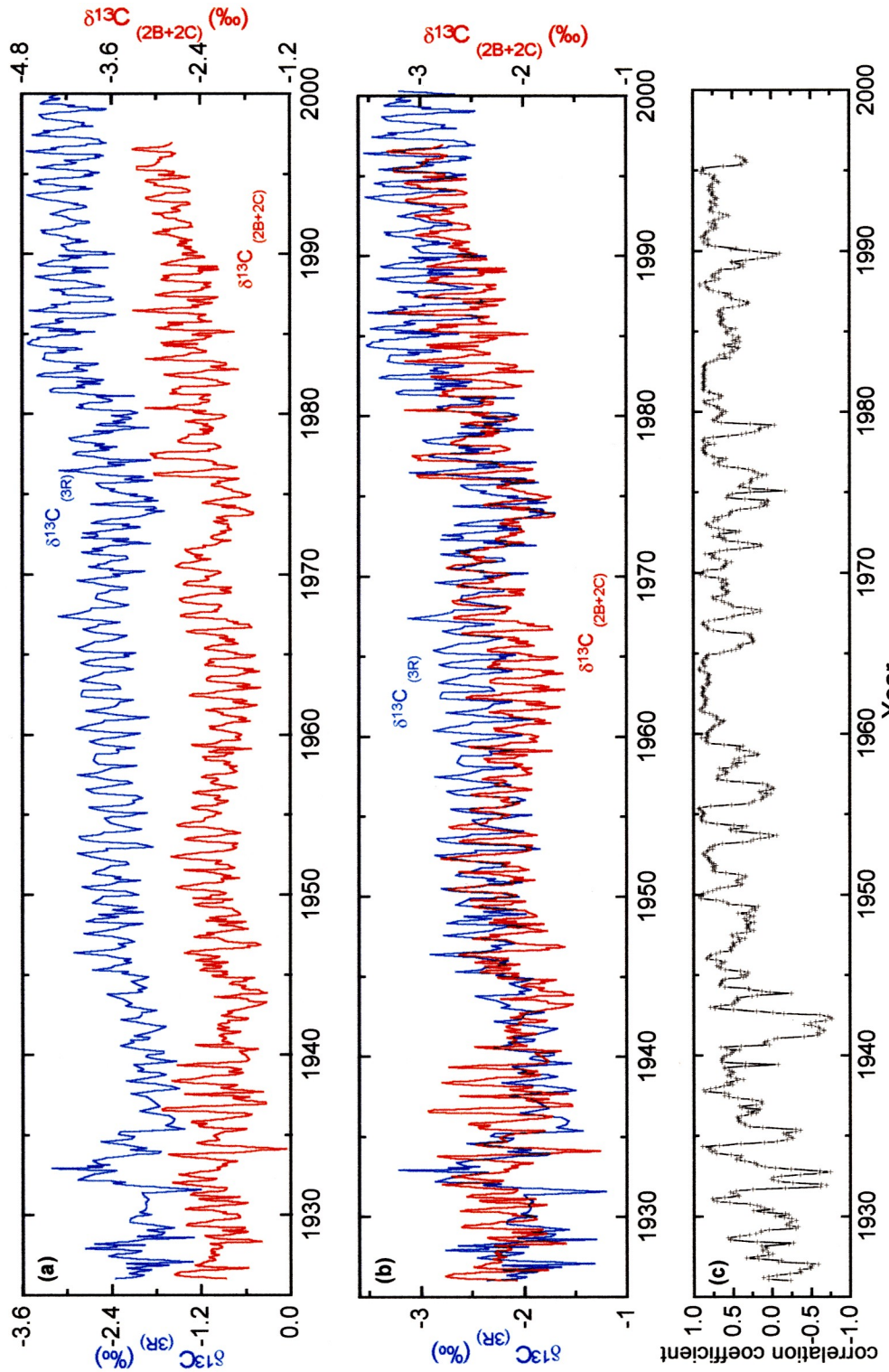

Fig. 5.7 (a) & (b) Comparison of $\delta^{13}C$ of core 2B+2C (in red) with core 3R $\delta^{13}C$ (in blue) for the period 1926-1997 at Rarotonga. **(c)** Moving correlation coefficient (1-year window) showing the correlation between 2B+2C $\delta^{13}C$ and 3R $\delta^{13}C$.

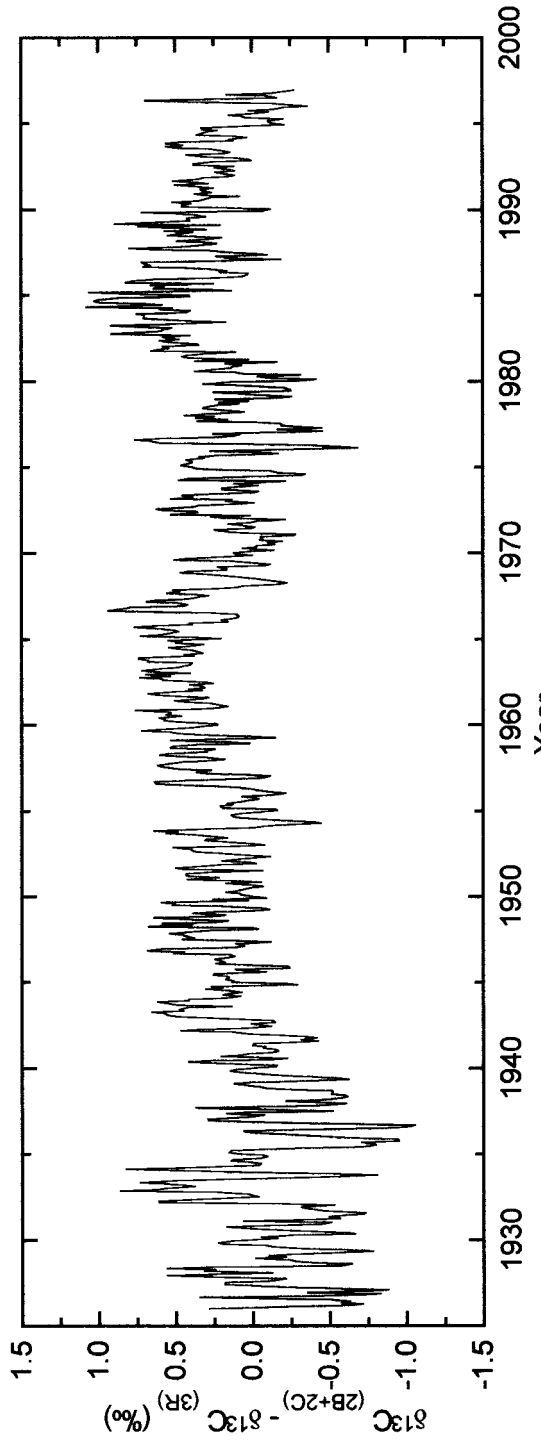

Fig. 5.8 The differences in $\delta^{13}C$ between the record 2B+2C and 3R ($\delta^{13}C_{2B+2C}$ - $\delta^{13}C_{3R}$) for the period 1926-1997 at Rarotonga.

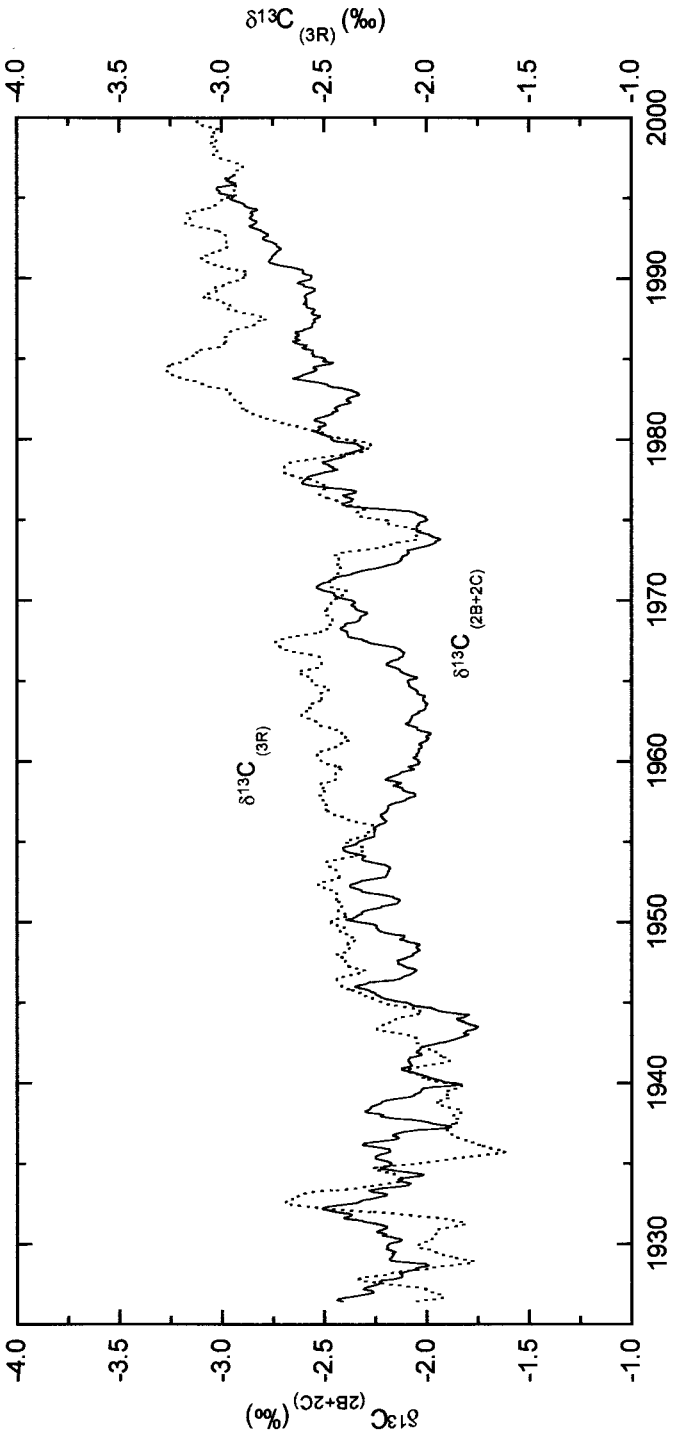

Fig. 5.9 Comparison of 12-month running average coral record of 2B+2C $\delta^{13}C$ (in solid line) with 3R $\delta^{13}C$ (in dotted line) from Rarotonga for the period 1926-1997.